



The Abdus Salam
International Centre for Theoretical Physics



2272-10

Joint ICTP-IAEA School on Synchrotron Applications in Cultural Heritage and Environmental Sciences and Multidisciplinary Aspects of Imaging Techniques

21 - 25 November 2011

SR-(micro/T)XRF for environmental and conservation studies

G. Pepponi

*Centre for Materials and Microsystems
Fondazione Bruno Kessler
Trento
ITALY*

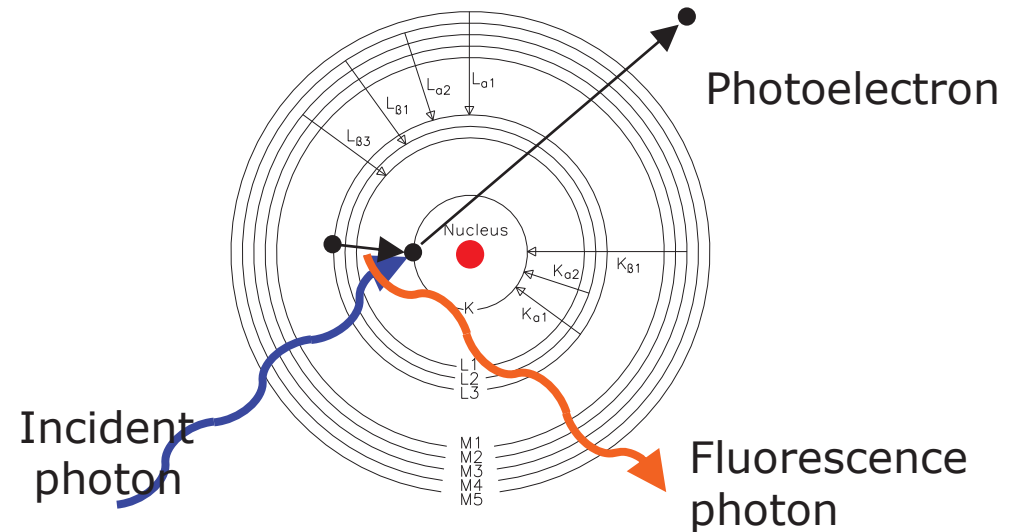
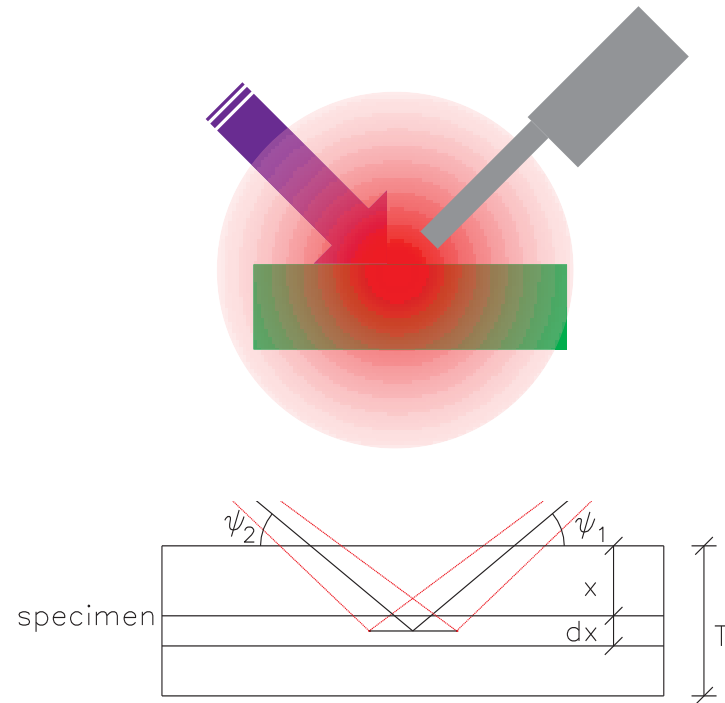
SR-(micro/T)XRF for environmental and conservation studies

Giancarlo Pepponi



Foundazione Bruno Kessler
Centre for Materials and Microsystems
Micro-Nano Analytical Laboratory
Via Sommarive 18, 38123 Povo (Trento) Italy
tel. +39 0461 314491
www.fbk.eu pepponi@fbk.eu

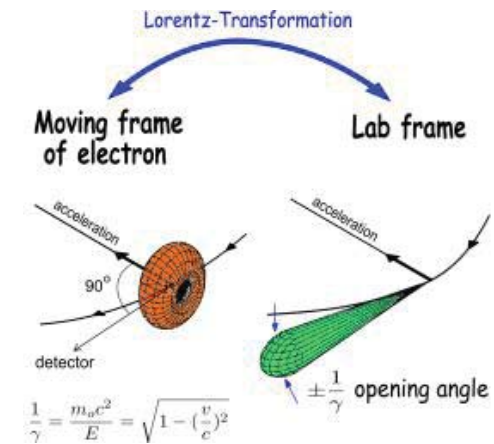
acknowledgement:
Norbert Zoeger – Atominstitut (TU Vienna)
Florian Meirer - FBK



$$I(E_{i,j,k}) = \frac{d\Omega_0 d\Omega_1}{4\pi} \int_0^t \int_{E_{edge,j}}^{E_{max}} \left[I_0(E_0) \exp\left(-\left(\frac{\mu}{\rho}\right)_{s,E_0} \rho_s \frac{x}{\sin \psi_0}\right) \exp\left(-\left(\frac{\mu}{\rho}\right)_{s,E_{i,j,k}} \rho_s \frac{x}{\sin \psi_1}\right) \right]$$

$$W_i \frac{\left(\frac{\tau}{\rho}\right)_{i,E_0}}{\sin \psi_0} \frac{(r_{i,j} - 1)}{r_{i,j}} \rho_s \omega_{i,j} p_{i,j,k} \mathcal{E}_{E_{i,j,k}} \left] dx dE_0 \right]$$

Synchrotron

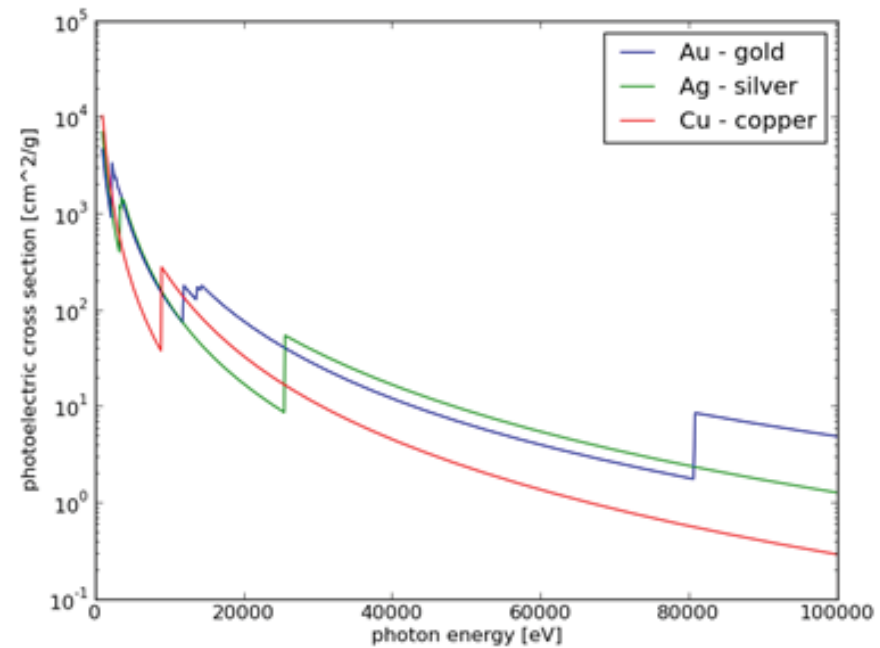


Higher flux:
 - faster measurements
 (scanning)

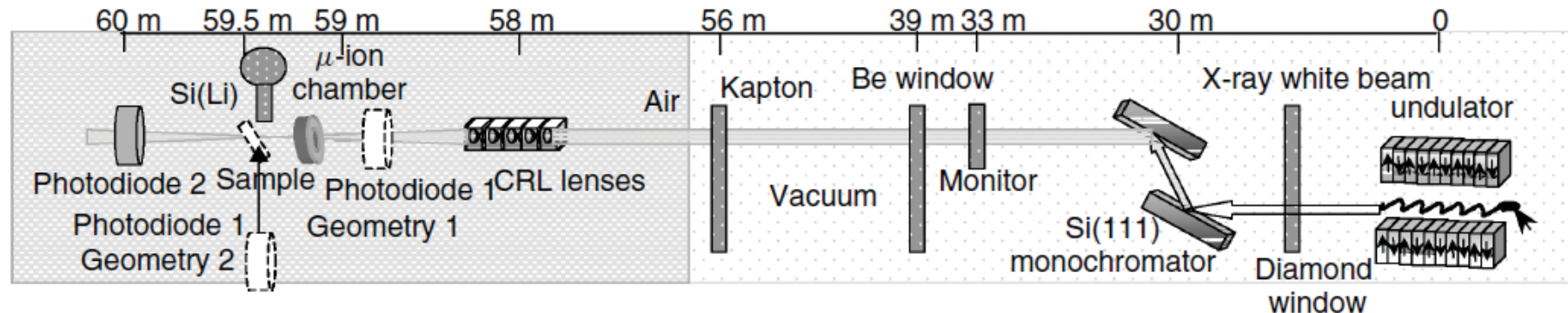
Natural collimation:
 -> high brilliance
 - micro (nano) spots

Polarisation:
 - better peak/background
 - magnetism

Wide spectral range:
 - selective excitation
 - excitation energy vs. sensitivity
 - energy scanning



Synchrotron – microXRF beamline example

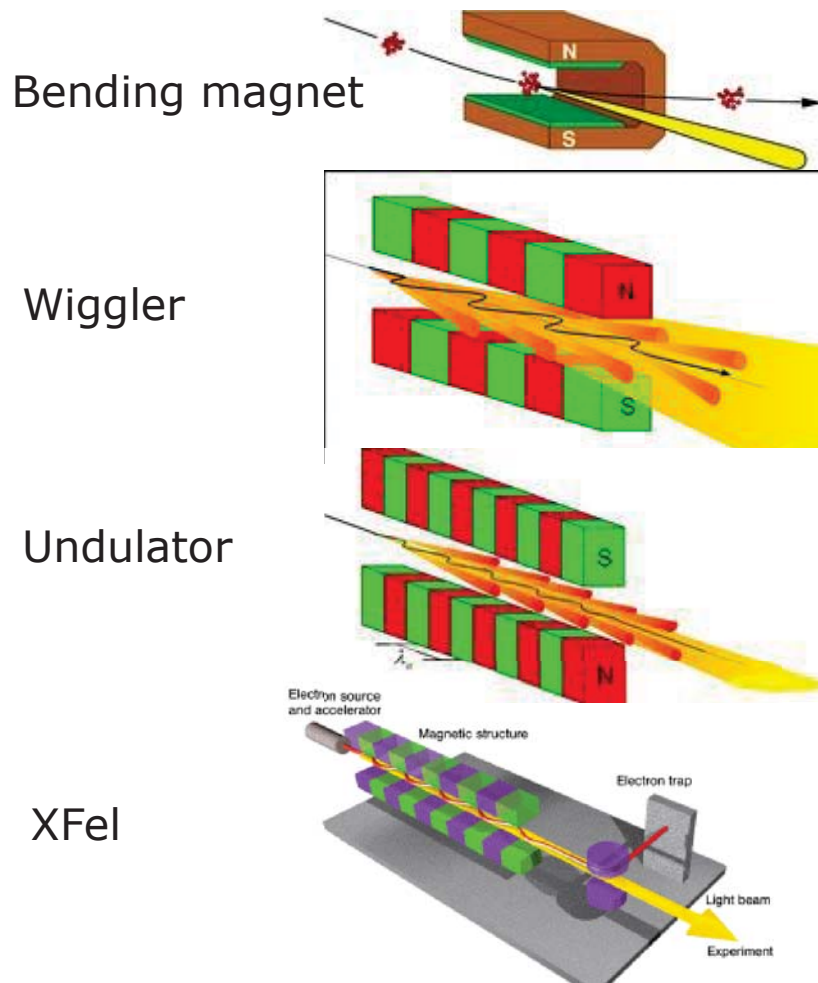


Schematic layout of the ID 18F experimental station. Photodiode 1 is either placed into the sample position if the sample is measured (geometry 1) or in front of the mini-ionisation chamber (geometry 2).

Somogyi, A., Drakopoulos, M., Vekemans, B., Vincze, L.,
 Simionovici, A. and Adams, F. *Nucl. Instrum. Methods B*
199, 559–564 (2003).

Synchrotron - sources

http://hasylab.desy.de/science/studentsteaching/primers/synchrotron_radiation/index_eng.html



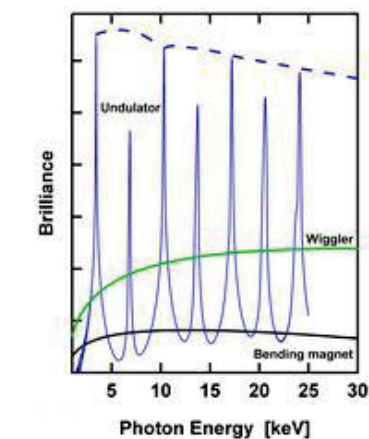
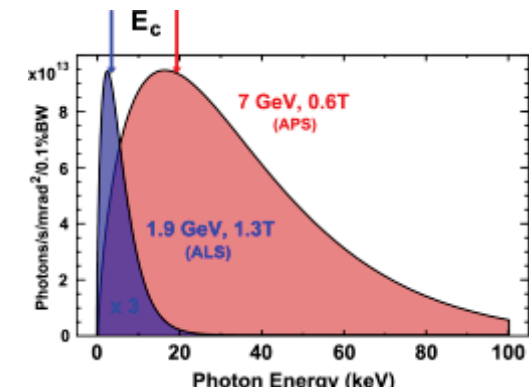
<http://xray.bmc.uu.se/spb/>

$$I \propto n$$

$$I \propto N$$

$$I \propto N^2$$

$$I \propto n^2$$



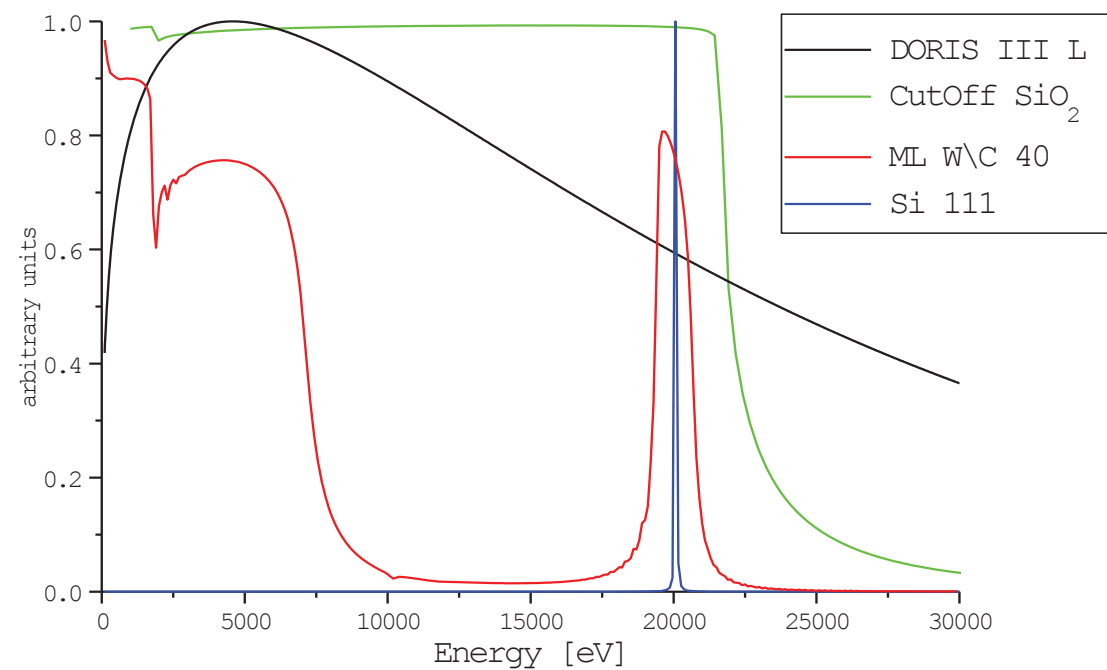
Spectral modifications

Mirrors – total reflection
cut-off, low-pass
(focussing)

Crystals – Bragg reflection
monochromators
 $\delta E/E \propto 10^{-3} - 10^{-4}$

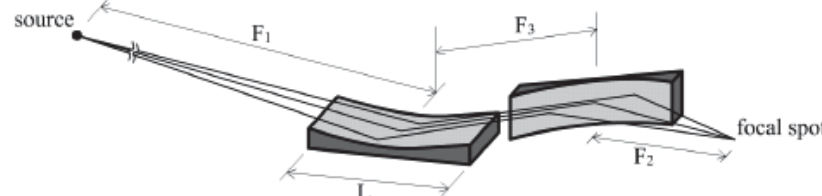
Multilayers – Bragg reflection
monochromators
 $\delta E/E \propto 10^{-2}$

Gratings – Bragg reflection
monochromators
 $\delta E/E \propto 10^{-3} - 10^{-4}$

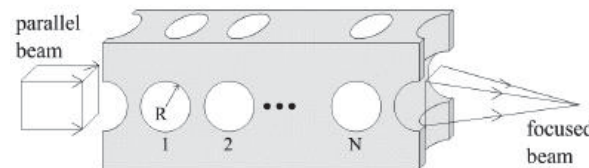


Focussing Optics

reflective:
Kirkpatrick-Baez



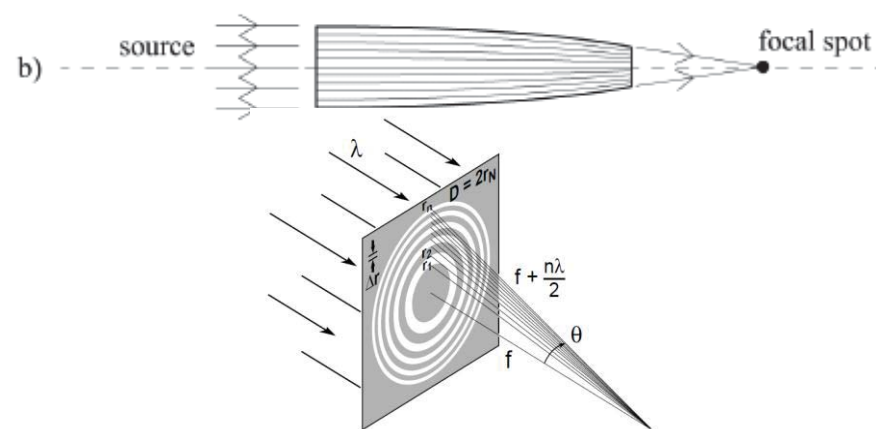
compound refractive lenses



monocapillaries



polycapillaries



zone plates

Flux density gain

Spot size

Energy range

Focal length

Alignment

XRF detectors



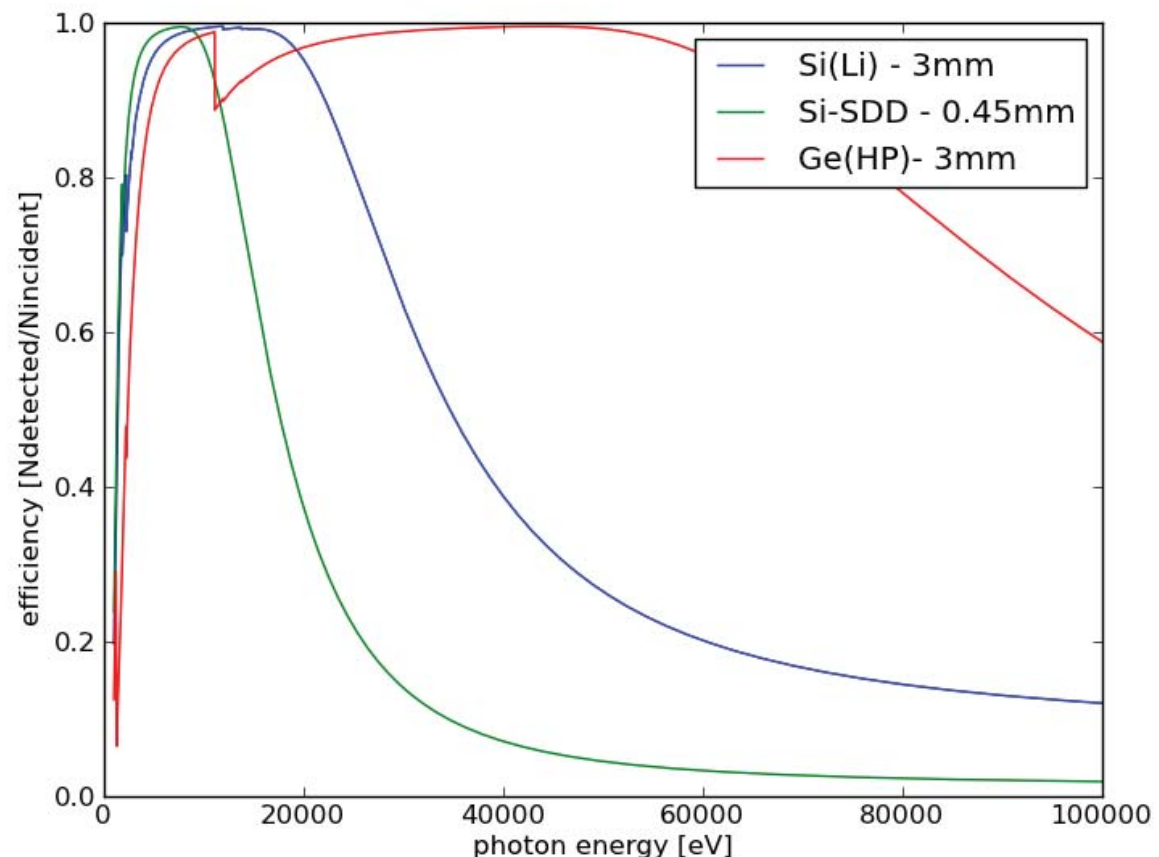
Silicon Drift Detectors:

- thin (efficiency)
- fast (up to 1Mcps)
- no LN2



Si(Li) – Ge(HP)

- thick (efficiency)
- not too fast (20-60 kcps)



XAS - detectors



7 element element



30 element

Lytle detector

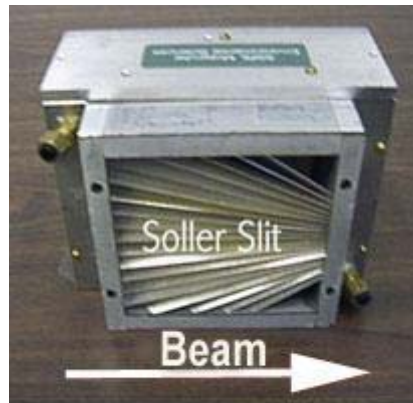


Figure 2. Soller Slit Position

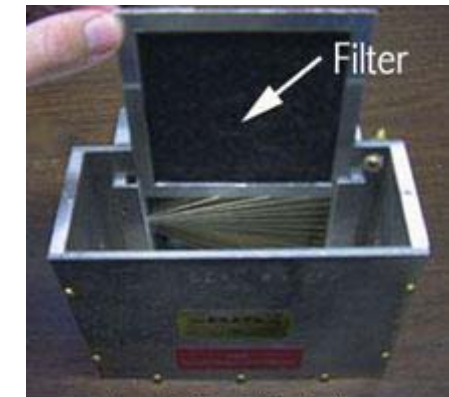
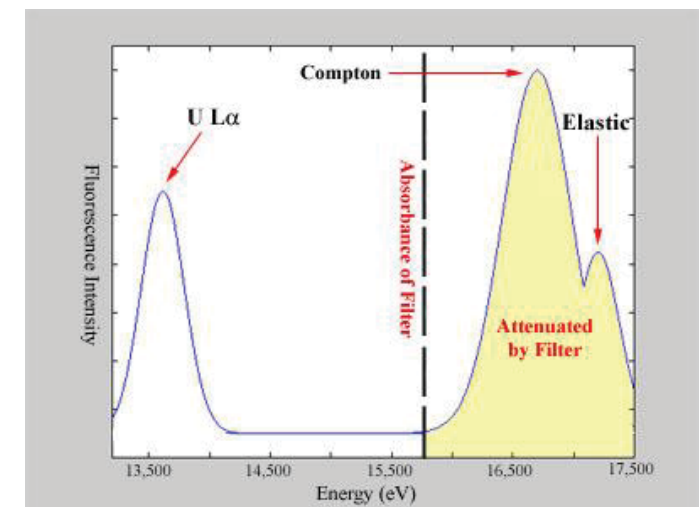
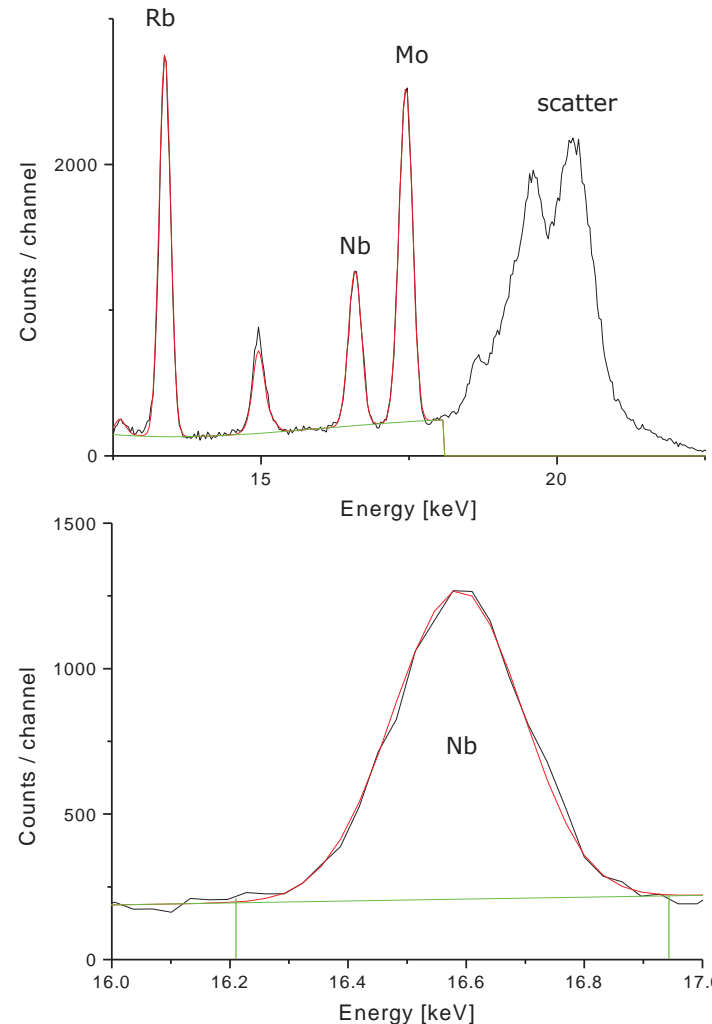


Figure 3. X-ray Filter Position

<http://ssrl.slac.stanford.edu/mes/xafs/index.html>



XRF – detection limits

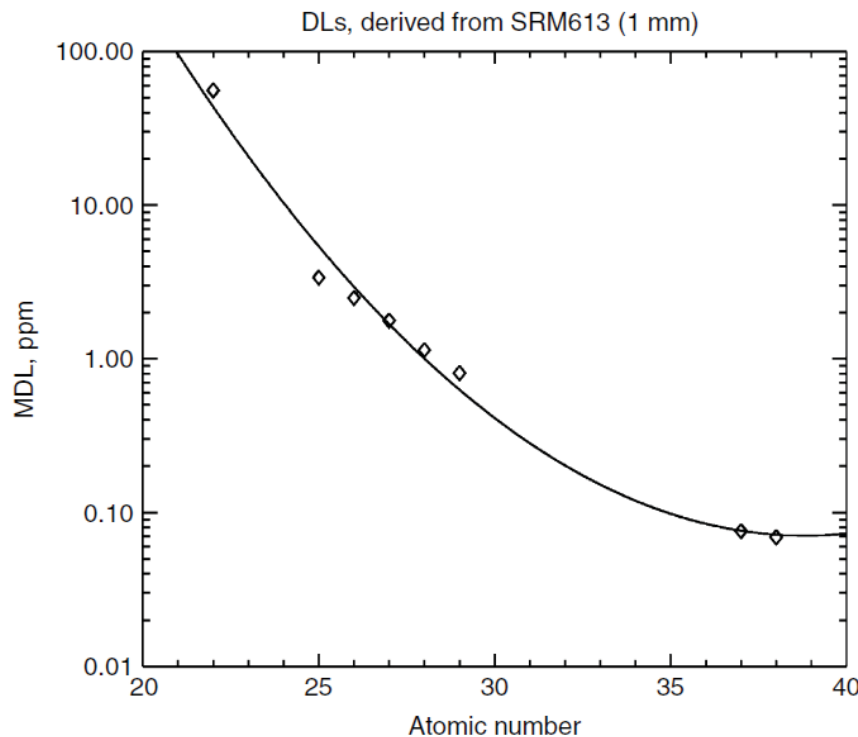
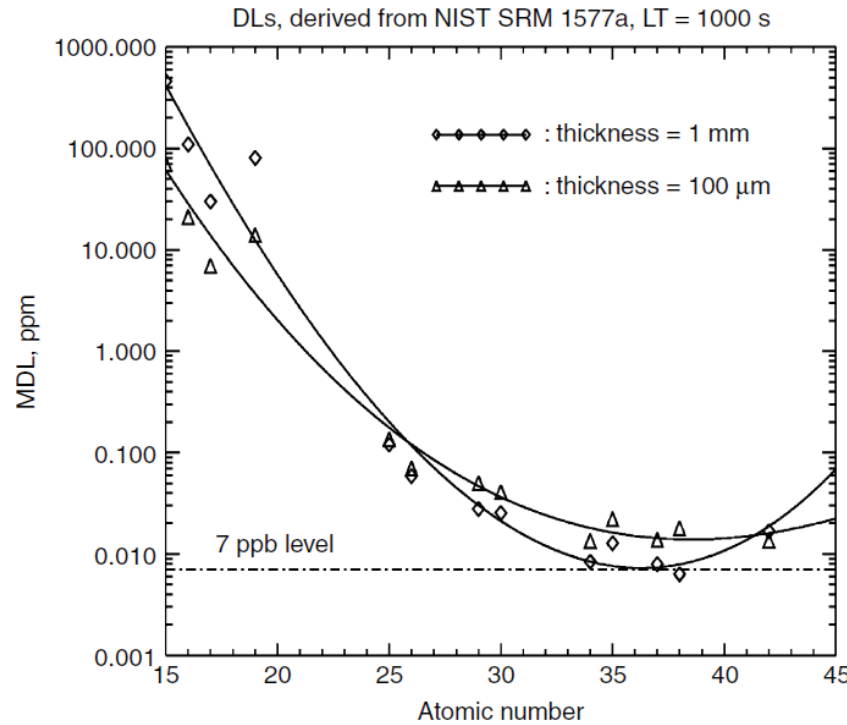


$$DL = 3 \frac{\sqrt{Background}}{Net} mass$$

$$DL \propto \sqrt{\frac{mass \cdot current}{time}}$$

Results usually normalised to
1000 sec measuring time

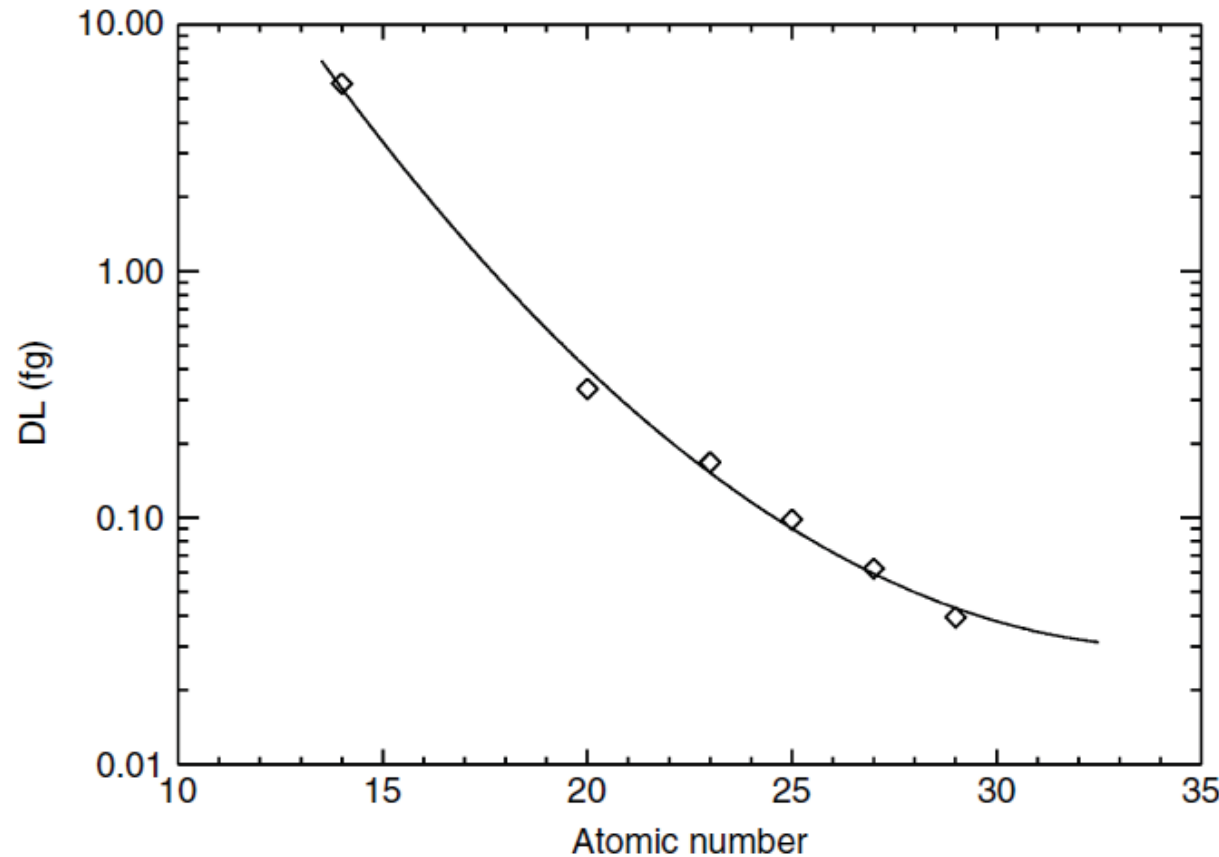
Synchrotron – detection limits



Relative detection limits with ID 18F using a 100 component compound reflective lens set at 21 keV at $2\mu\text{m} \times 2\mu\text{m}$ in biological material (NIST SRM 1577a, bovine liver) and NIST 613 glass SRM 613 (live time measurement of 1000 s).

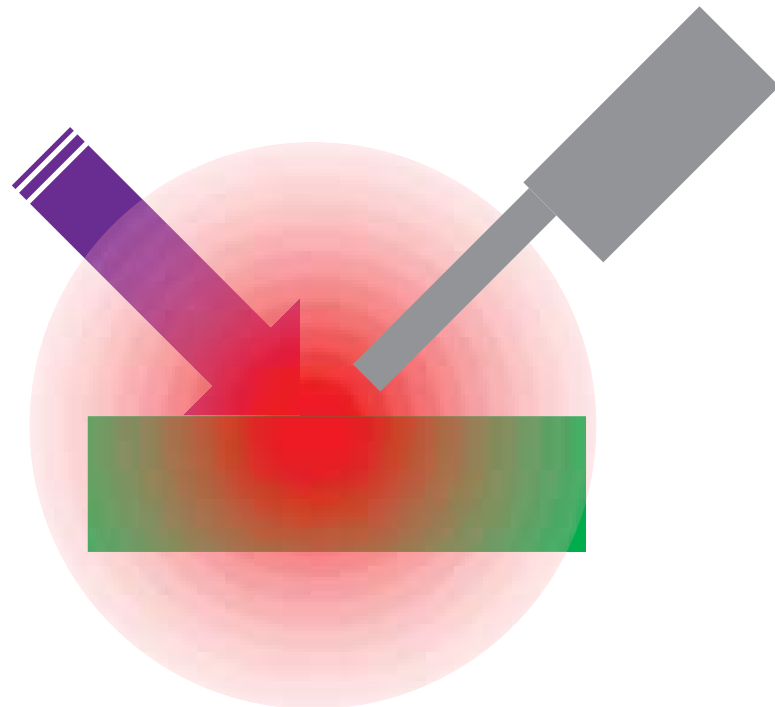
Somogyi, A., Drakopoulos, M., Vincze, L., Vekemans, B., Camerani, C., Janssens, K., Snigirev, A. and Adams, F. *X-ray Spectrom.* **30**, 242–252

Synchrotron – detection limits

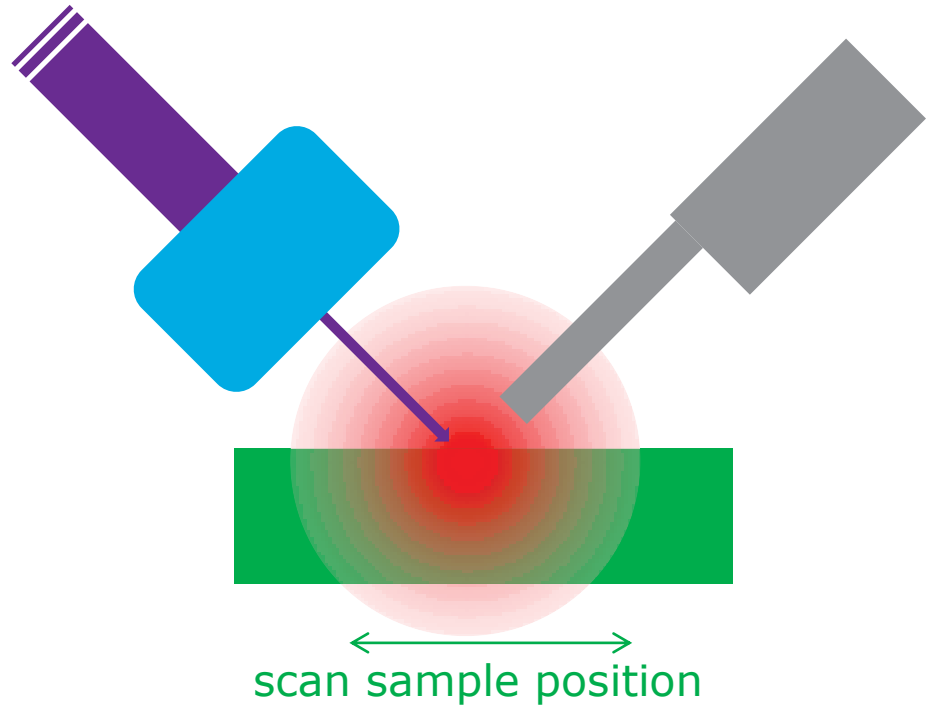


Absolute detection limits with ESRF (ID 13), 21 keV monochromatic radiation at $2\mu\text{m} \times 2\mu\text{m}$ (live time measurement of 100 s). Adapted from Somogyi *et al.* (2001)

Micro - XRF



- homogeneous sample (assumed – spinning)
- averaged information
- LD: ppm → ppb

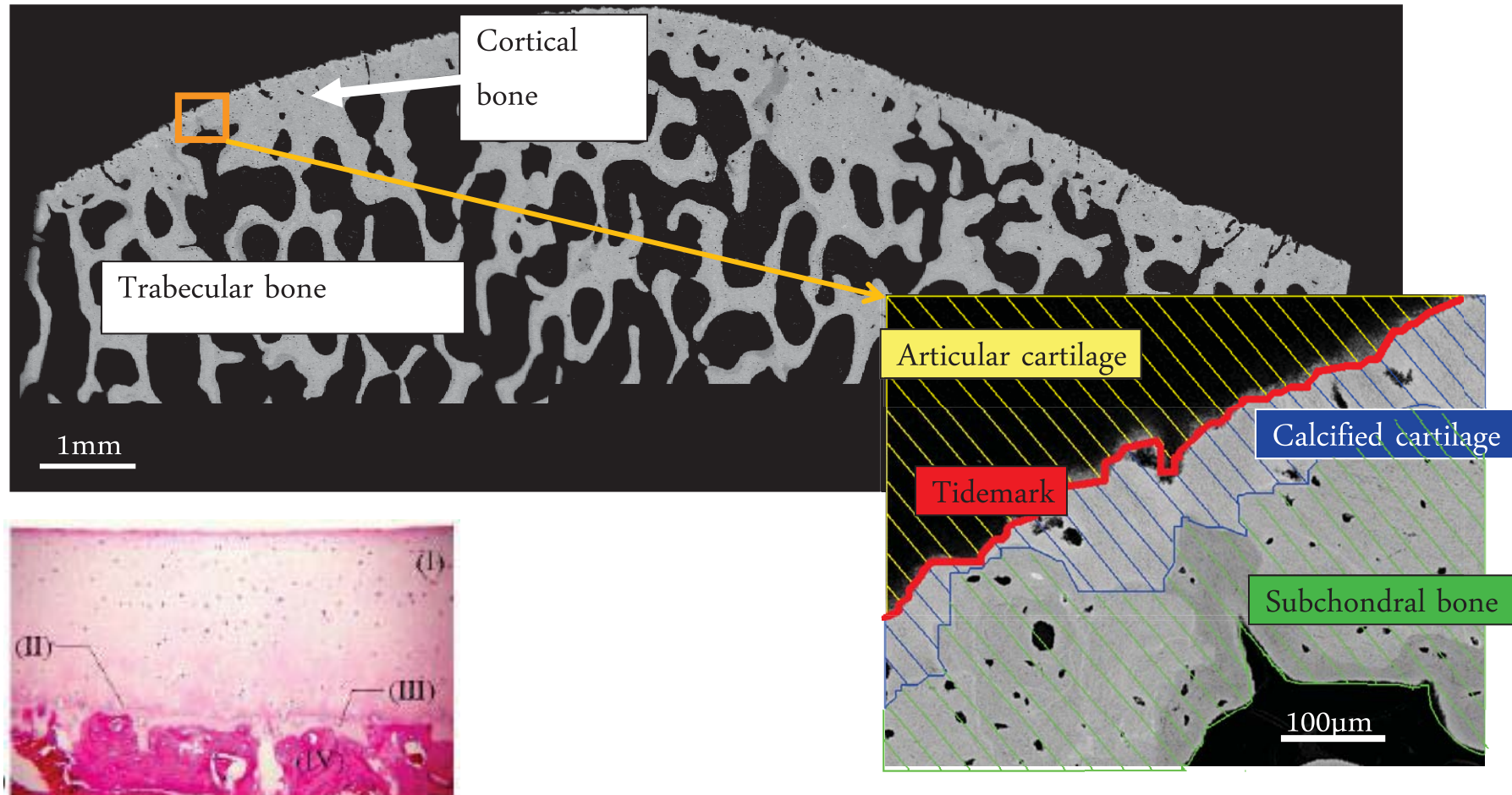


- detect inhomogeneities in sample
- local information → imaging
- LD: ppm → ppb ???
- improved signal to background ratio ?
- much more information
? data analysis ?

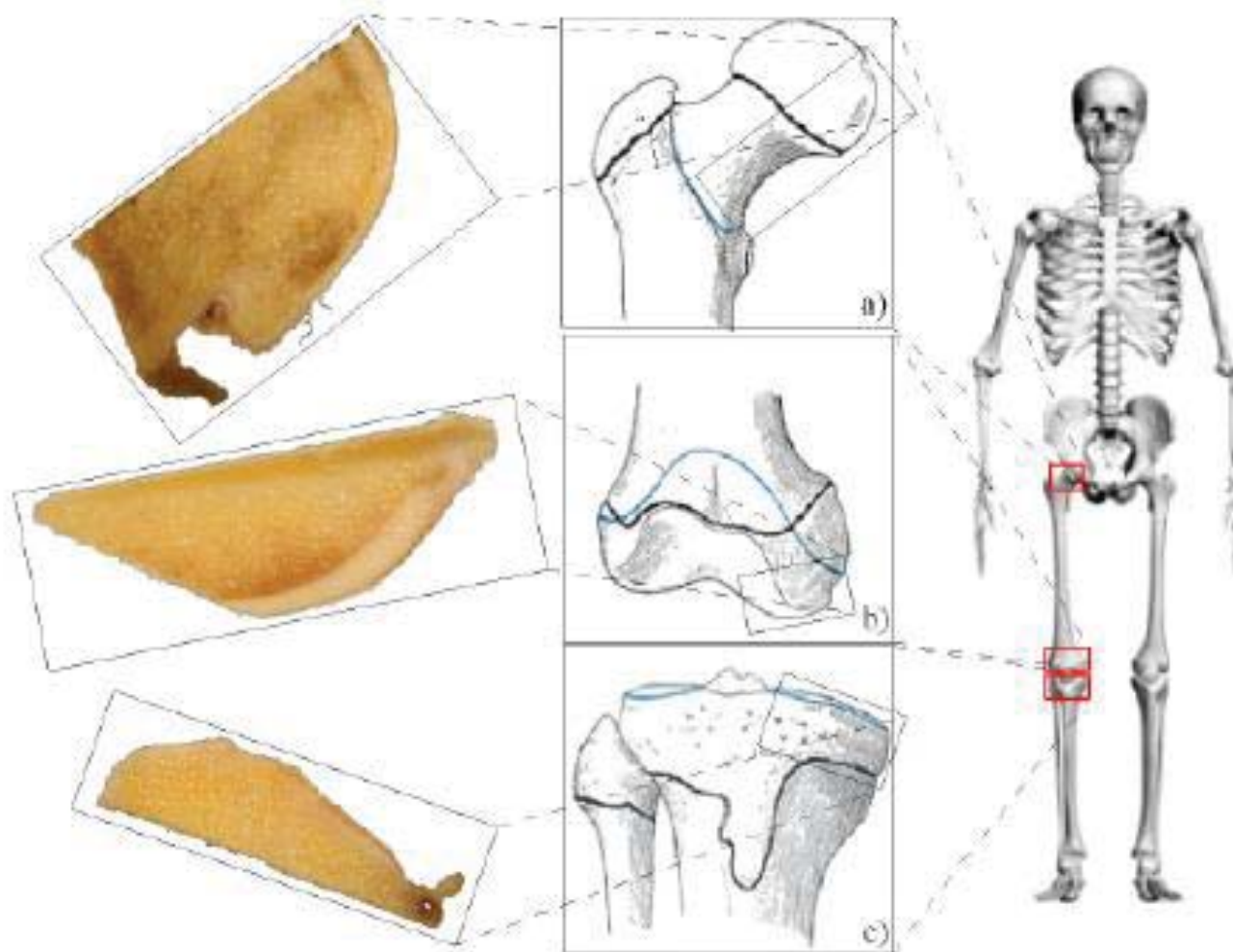
microXRF – example – lead in bone

Most of the work done by Norbert Zoeger for his PhD

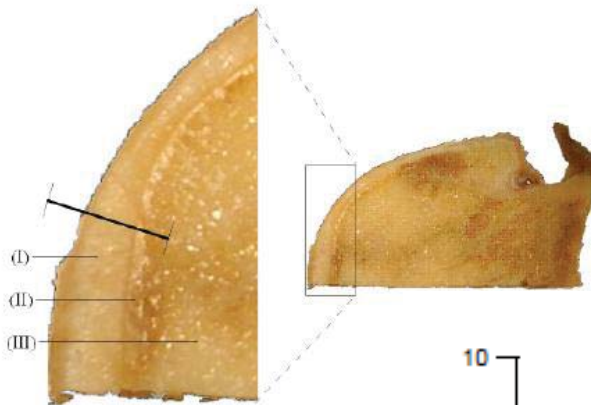
Backscattered Electron Image (BE), Patella



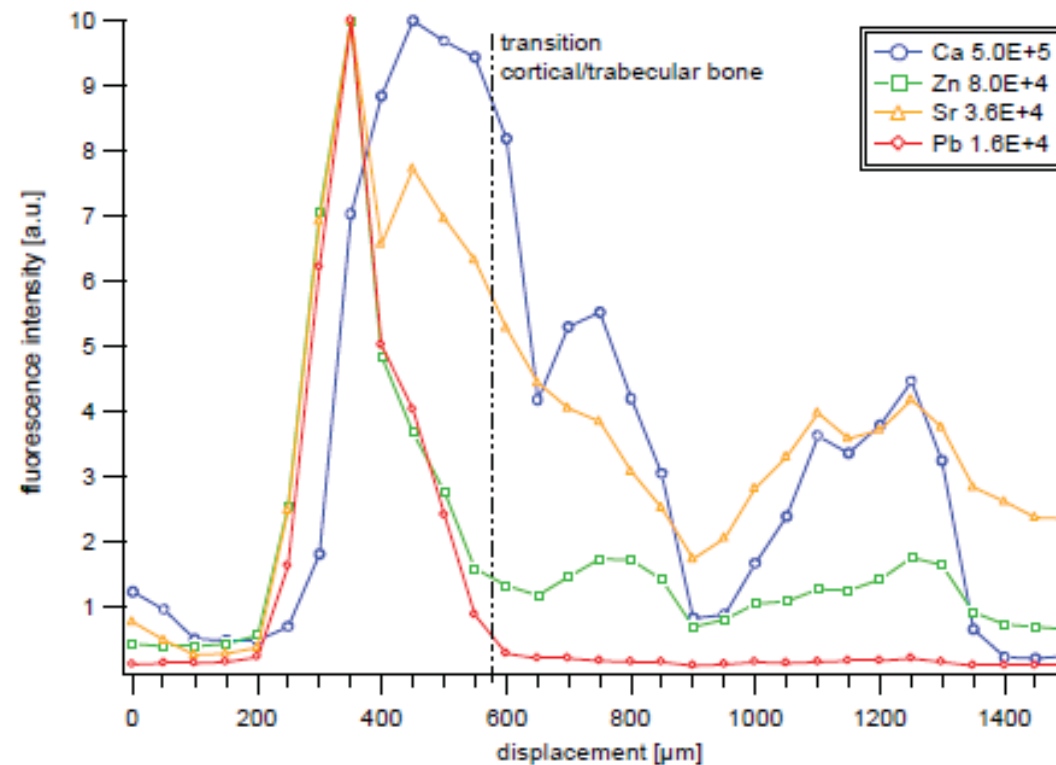
microXRF – example – lead in bone



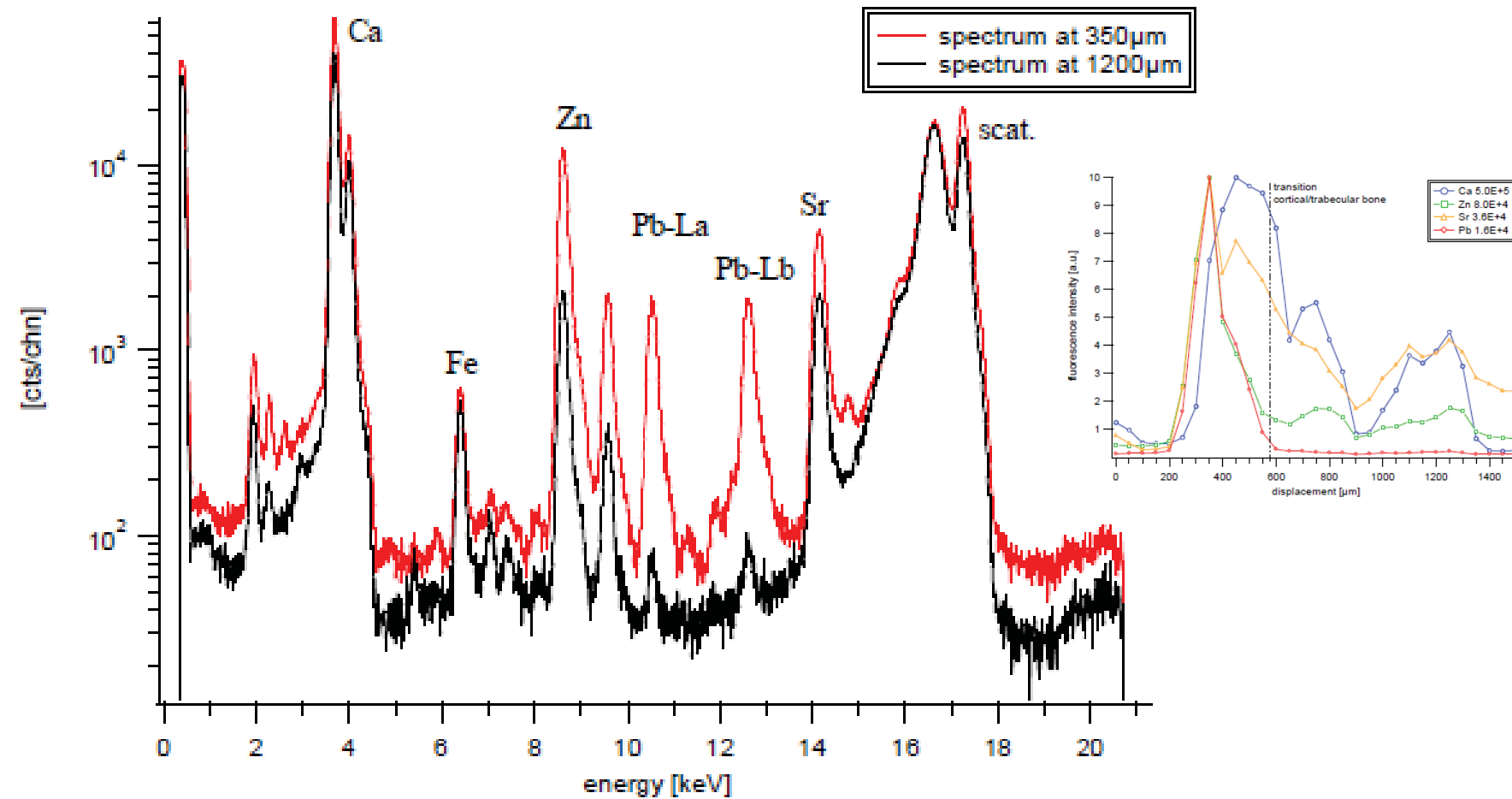
microXRF – example – lead in bone



1D scan
mm thick piece

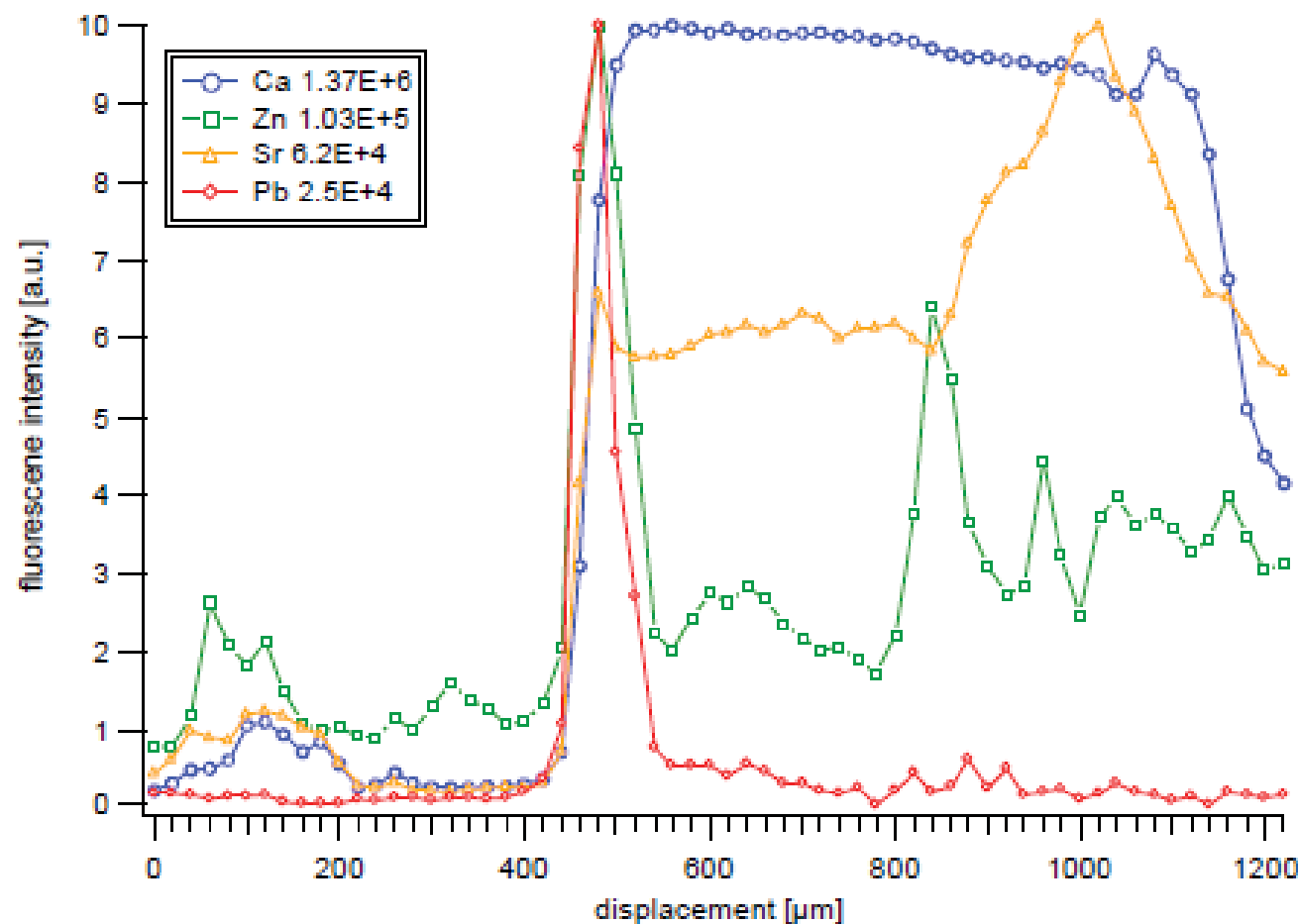


microXRF – example – lead in bone

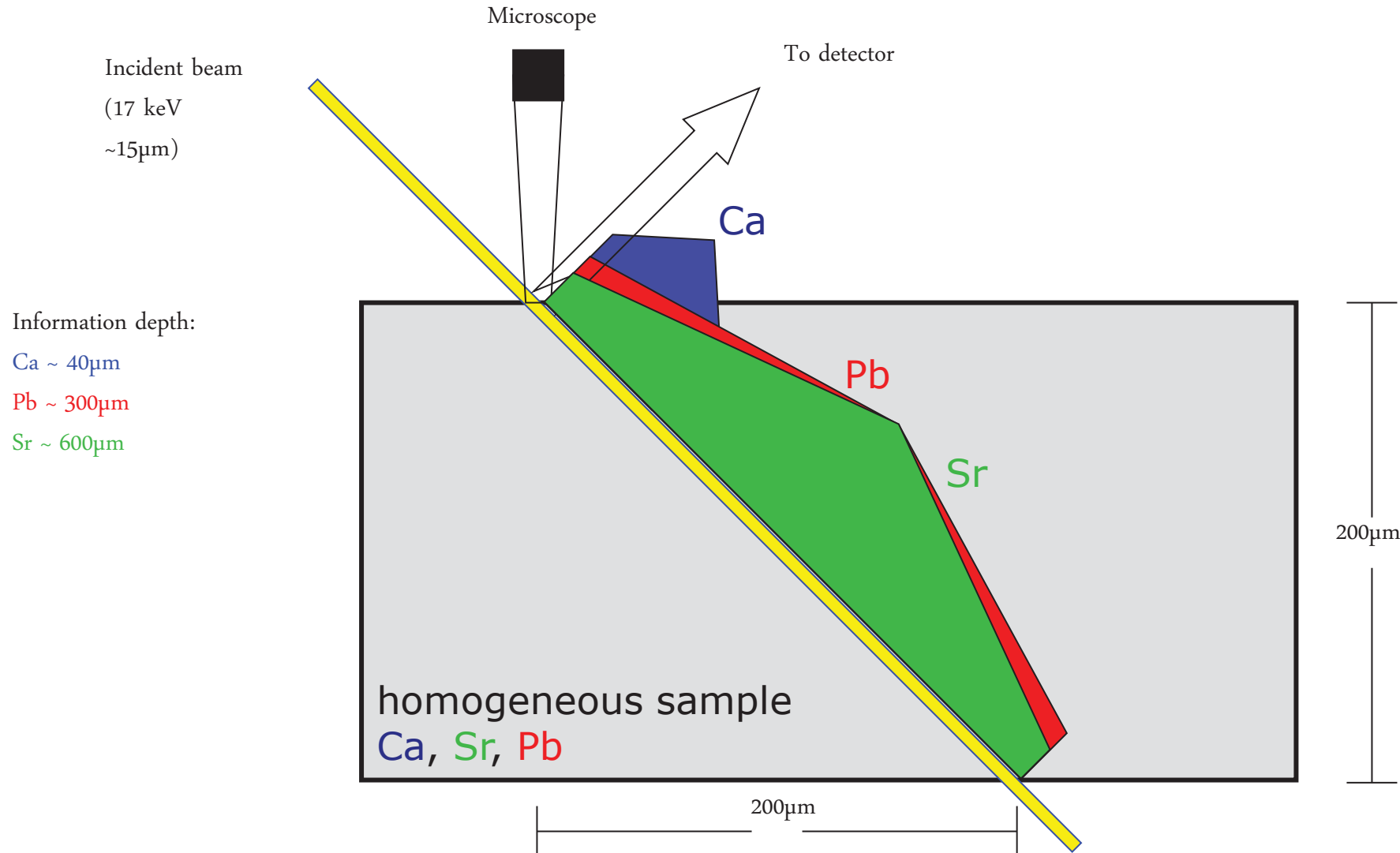


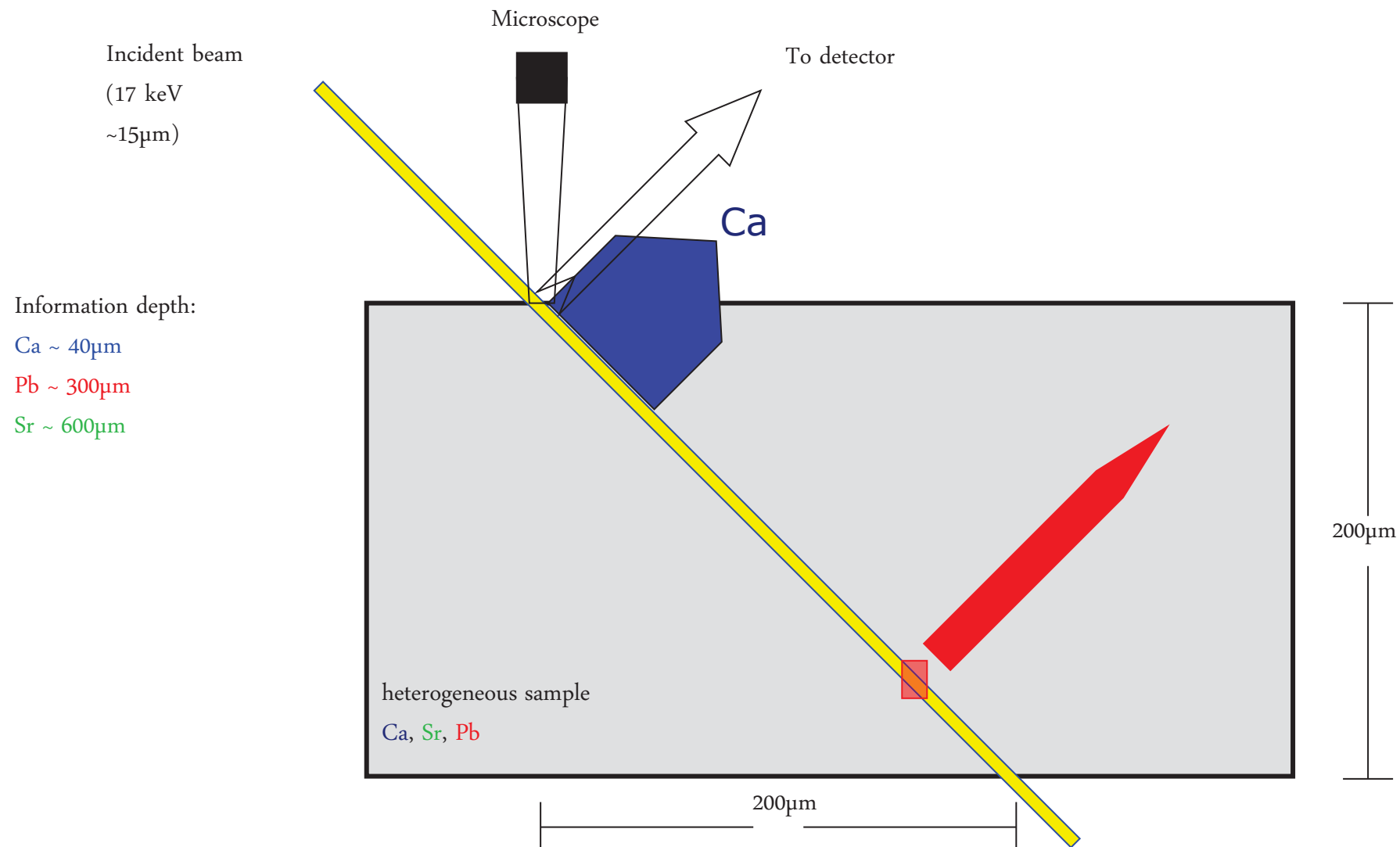
microXRF – example – lead in bone

1D scan
 200 μm thick piece



microXRF – artifacts





Why 3D?



Because 2D projection can be misleading.

Confocal set-up – hasylab L

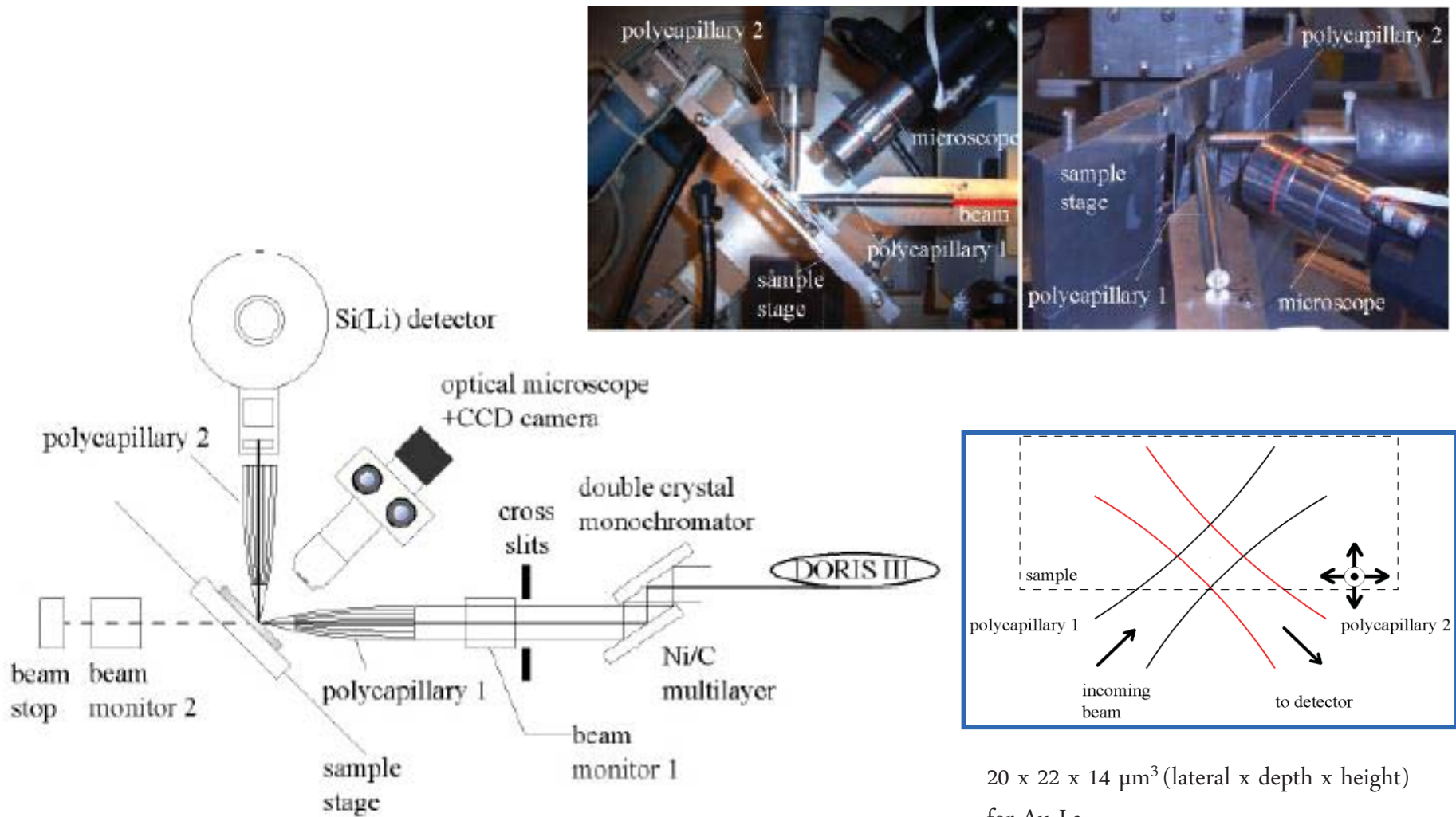
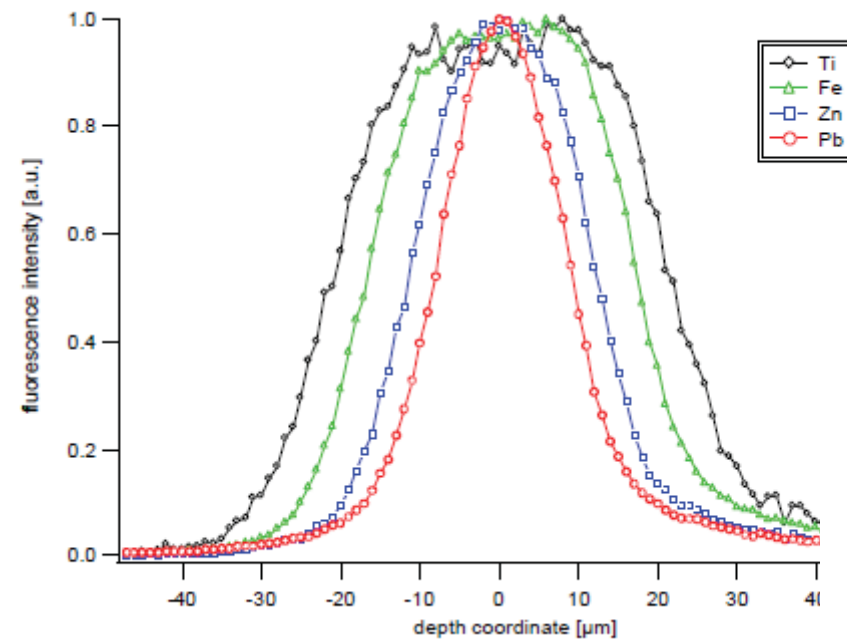


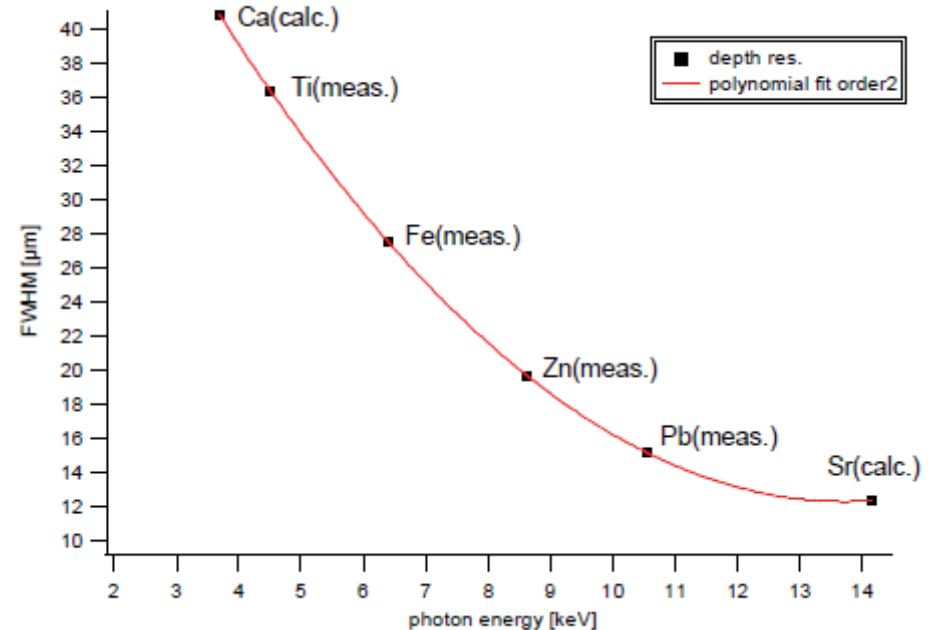
Figure 7.16: Scheme of the confocal setup at HASYLAB, beamline L

Confocal set-up – hasylab L

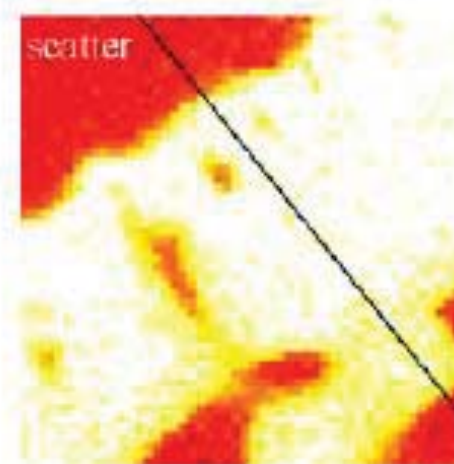
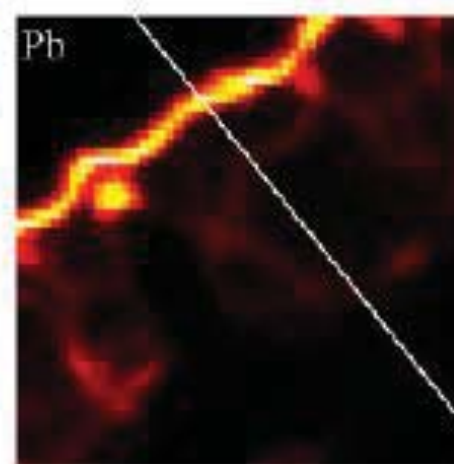
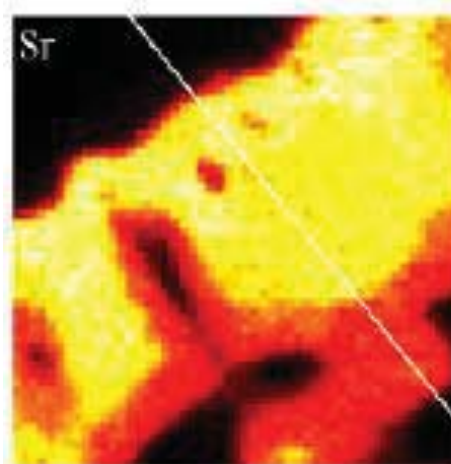
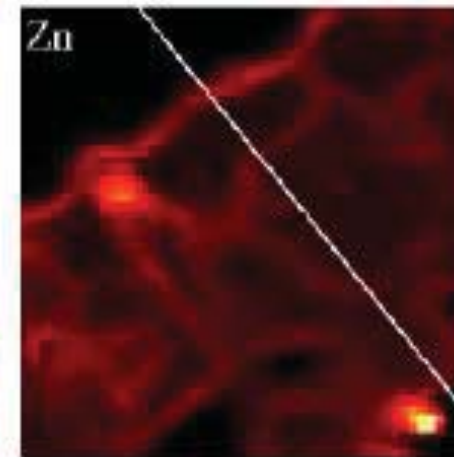
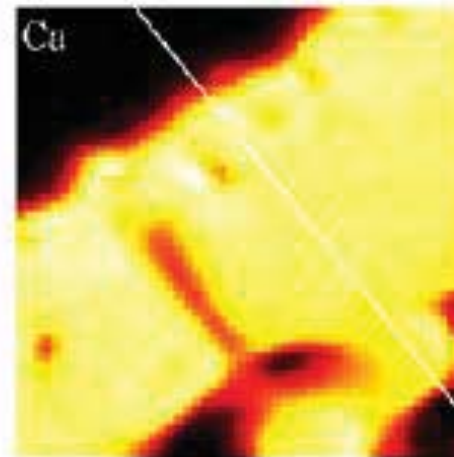
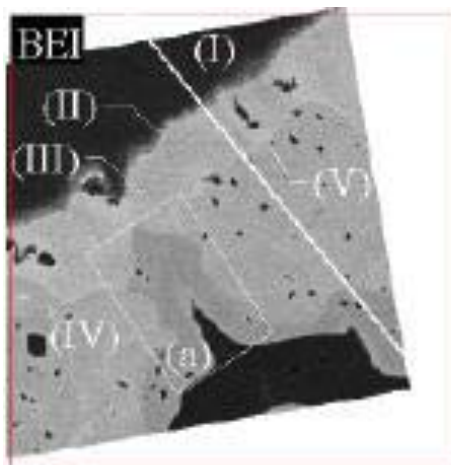


Detection volume

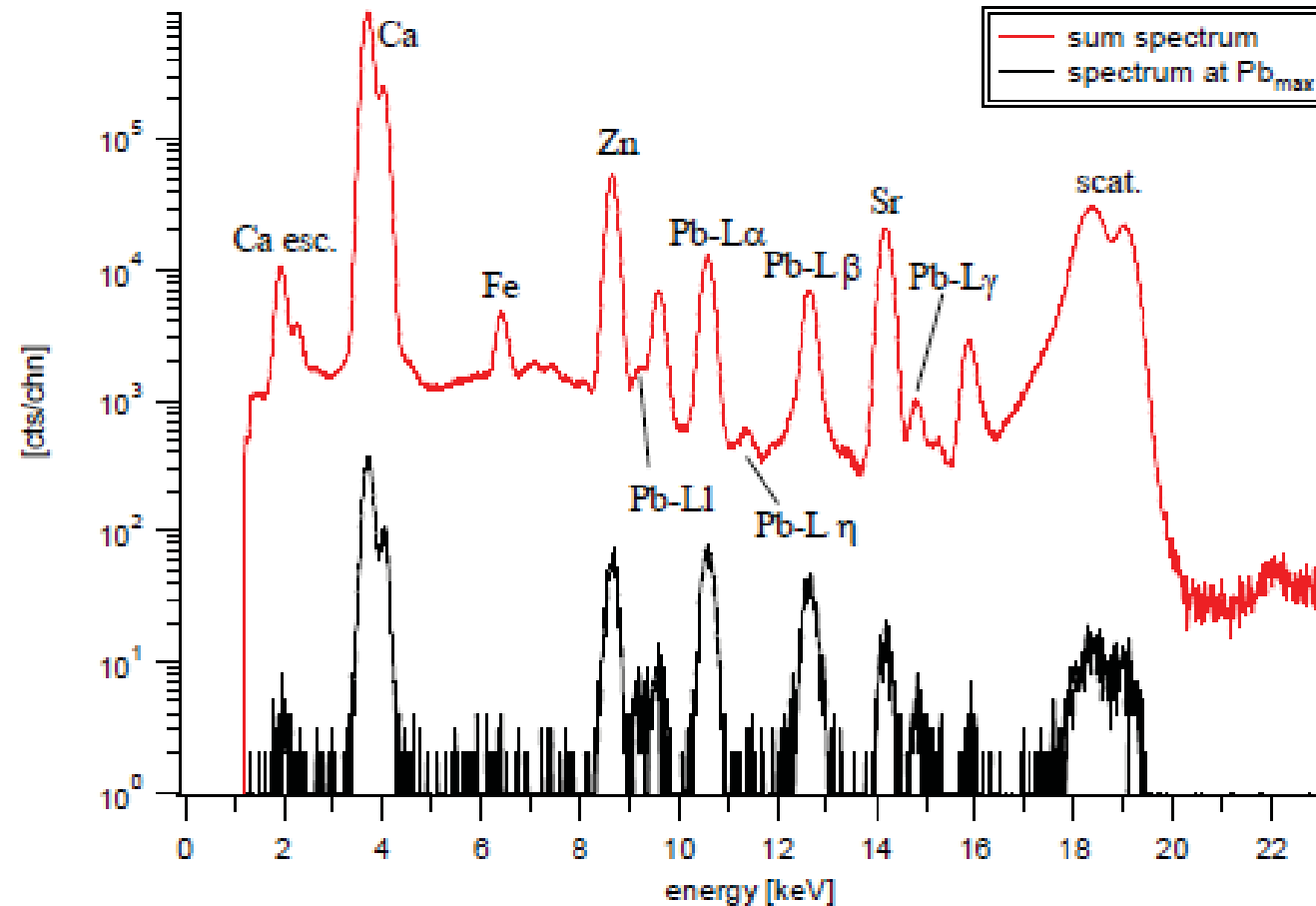
spatial resolution



Confocal set-up – hasylab L

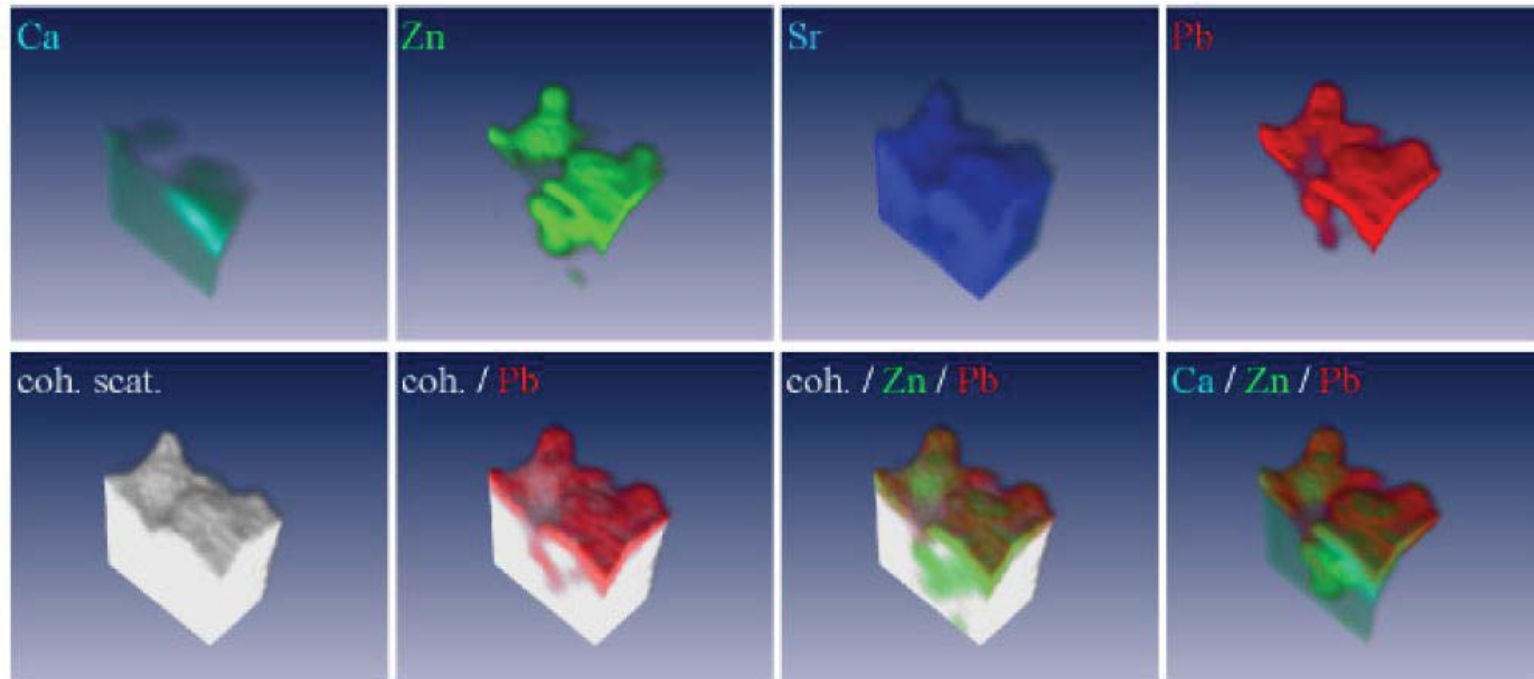


Confocal set-up – hasylab L



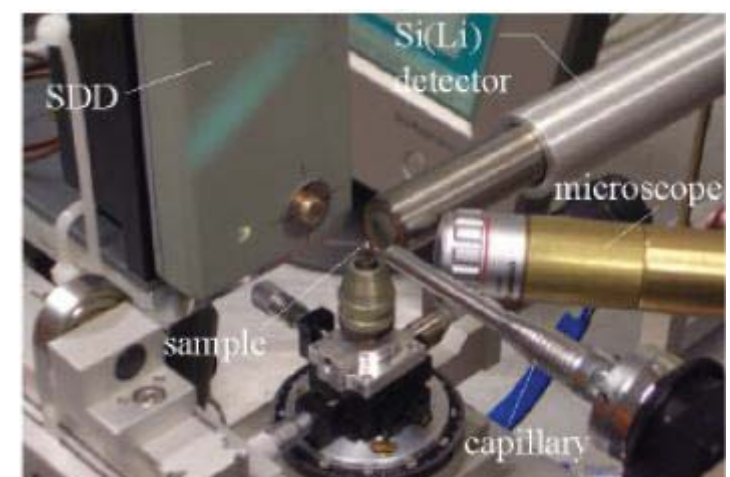
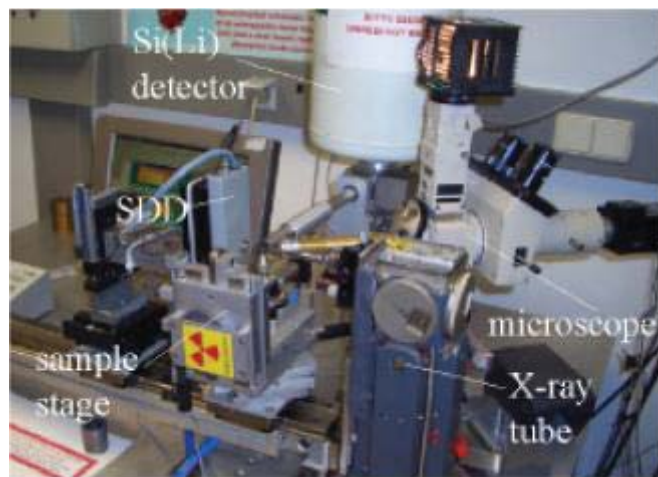
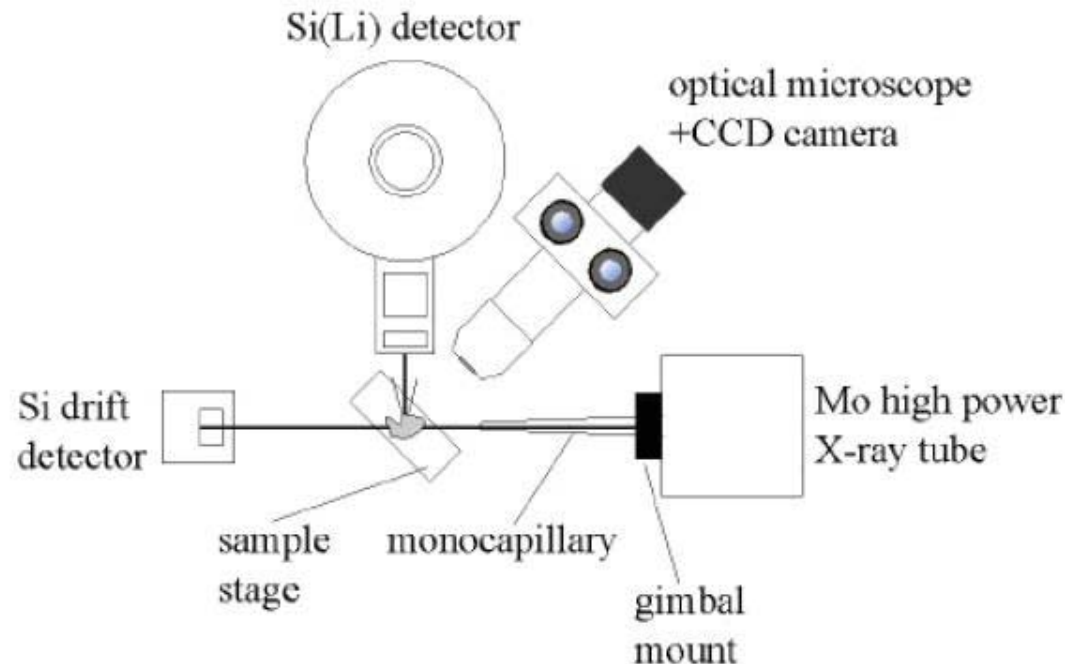
all (2601) fluorescence spectra from the area scan (red) compared with the single spectrum at the maximum of Pb (black), obtained in 5s measuring time

Confocal set-up – hasylab L



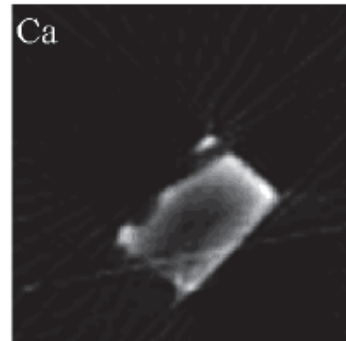
Three-dimensional element distribution in human patella

Tomo set-up – ANKA

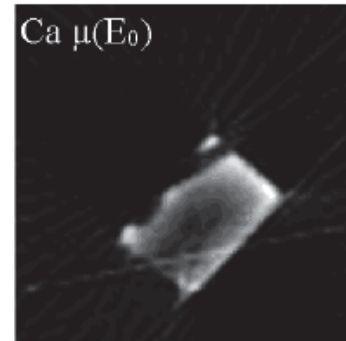


Tomo set-up – ANKA

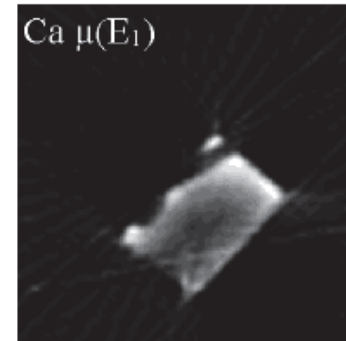
Ca



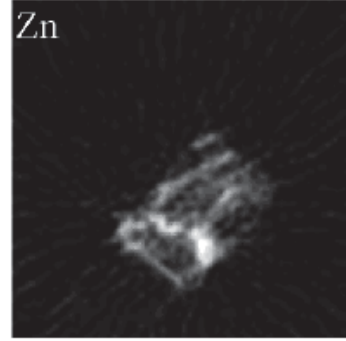
Ca $\mu(E_0)$



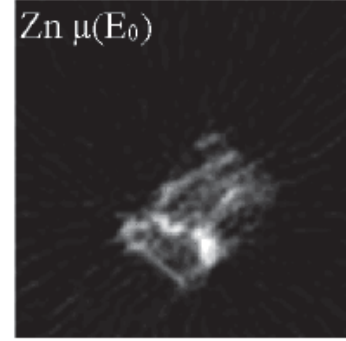
Ca $\mu(E_1)$



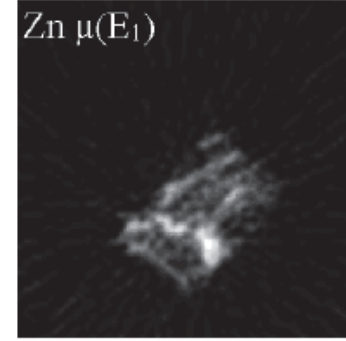
Zn



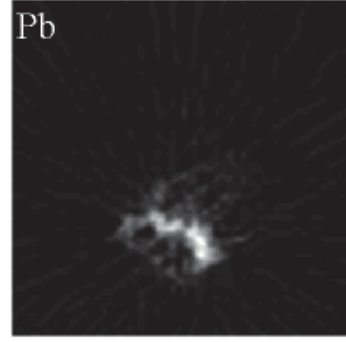
Zn $\mu(E_0)$



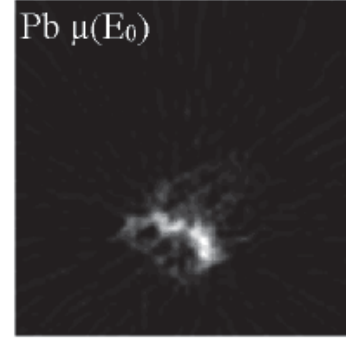
Zn $\mu(E_1)$



Pb



Pb $\mu(E_0)$



Pb $\mu(E_1)$

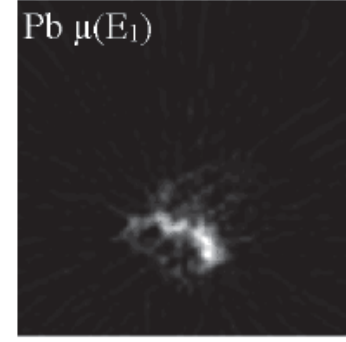


Figure 6

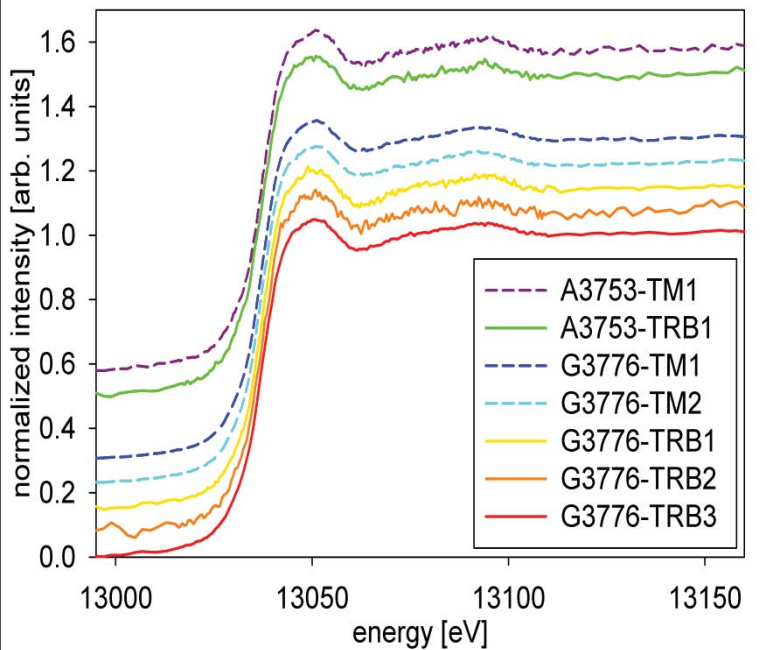


Figure 6: Comparison of XANES spectra recorded at different tidemark (TM) positions and different regions in the trabecular bone (TRB) of the human patella (G3776) and femoral head (A3753) sample [2].

Figure 7

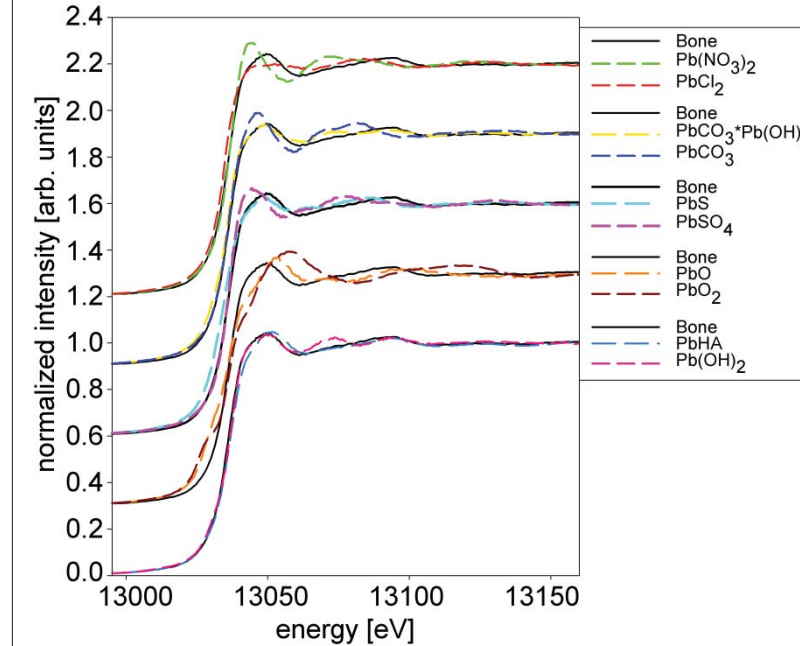
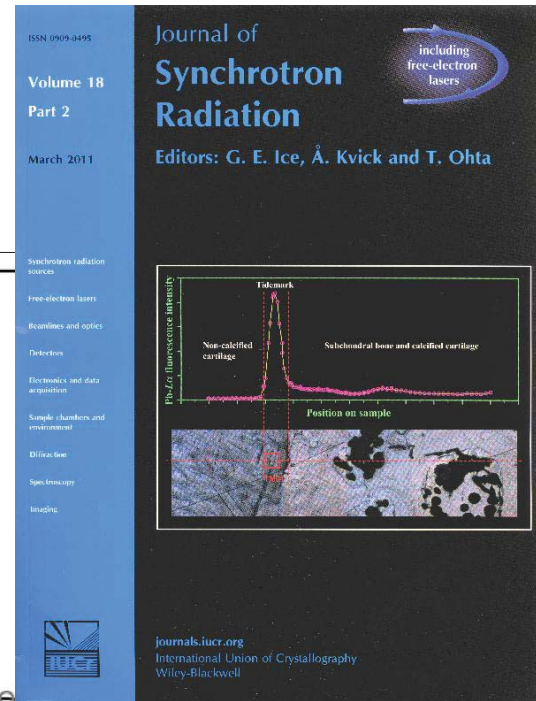
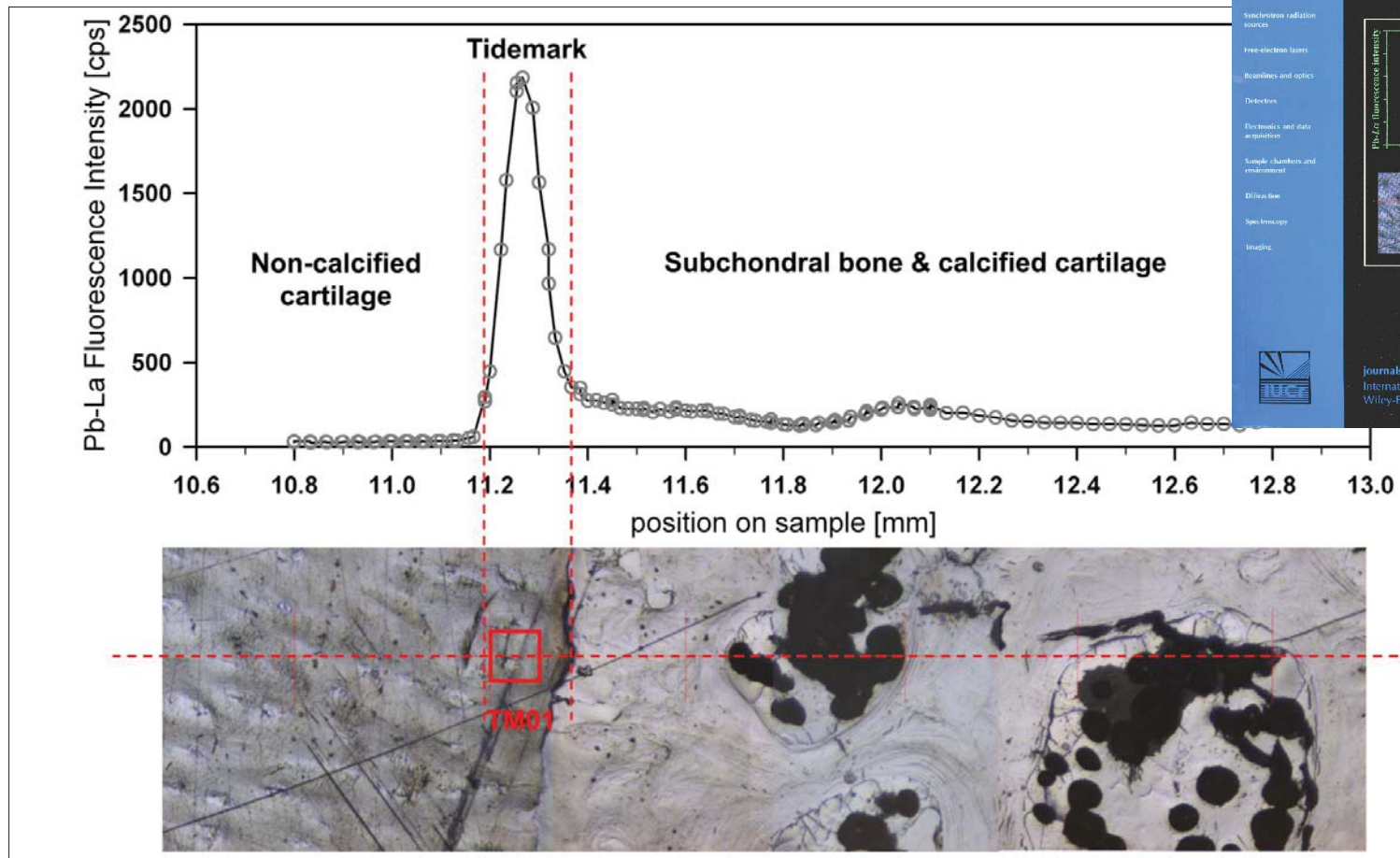
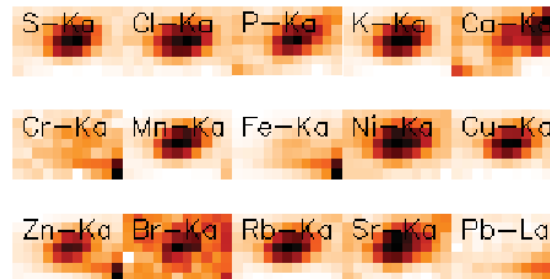
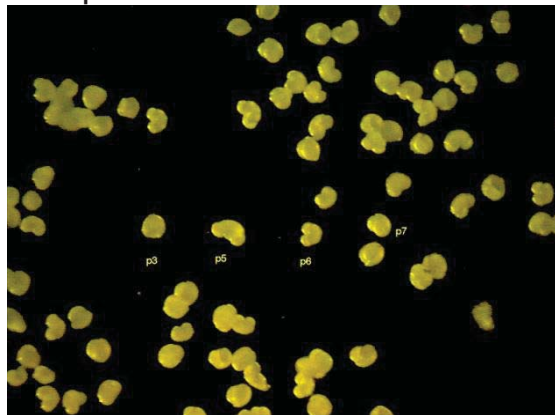


Figure 7: Comparison of bone XANES spectra (black) - because TM and TRB spectra of Fig. 6 show no differences they have been merged for further evaluation - with spectra of reference compounds [2].

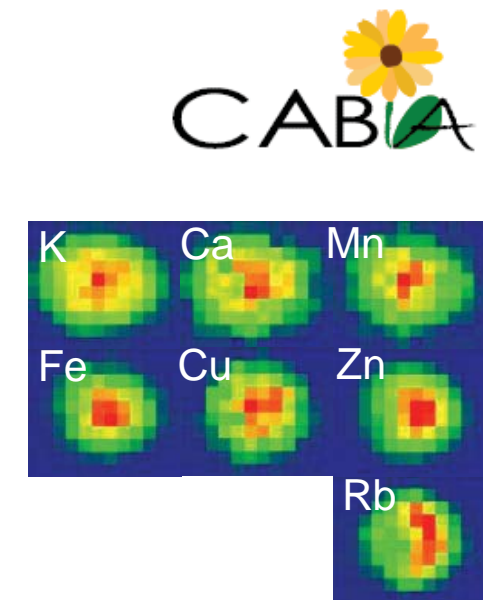


March 2011
cover

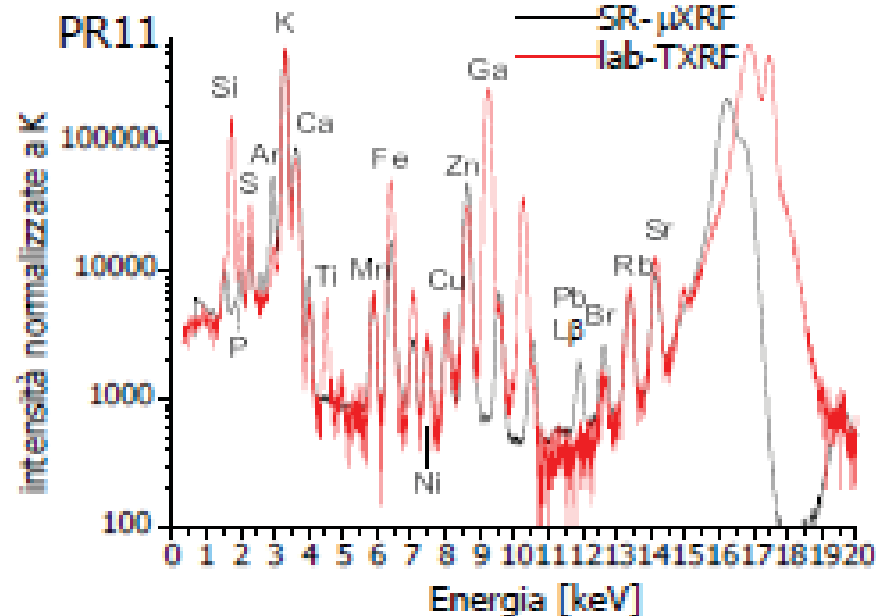
Sample PR11



Polycapillary micro-XRF



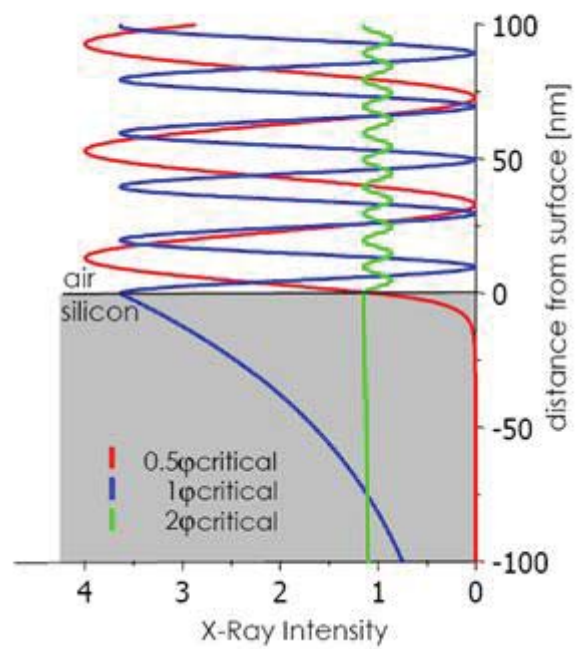
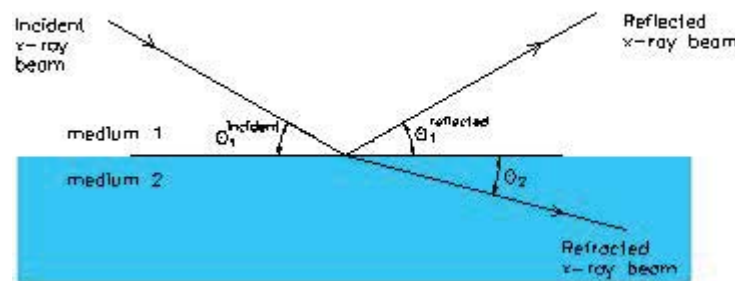
confocal micro-XRF



TXRF

Total Reflection X-Ray Fluorescence

Total external reflection



$$n \text{ (x-ray range)} = 1 - \delta - i\beta$$

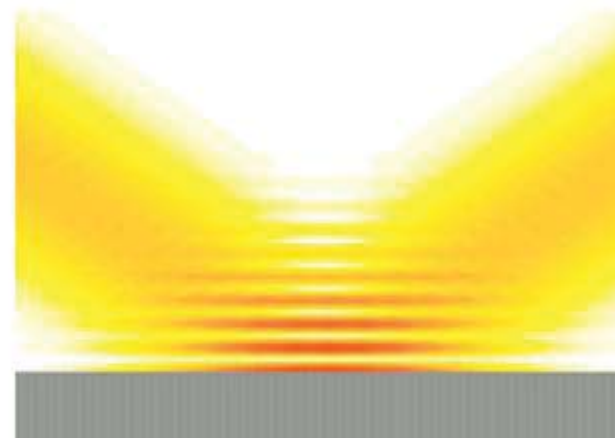
$$\delta \sim 10^{-6} \quad \beta \sim 10^{-8}$$

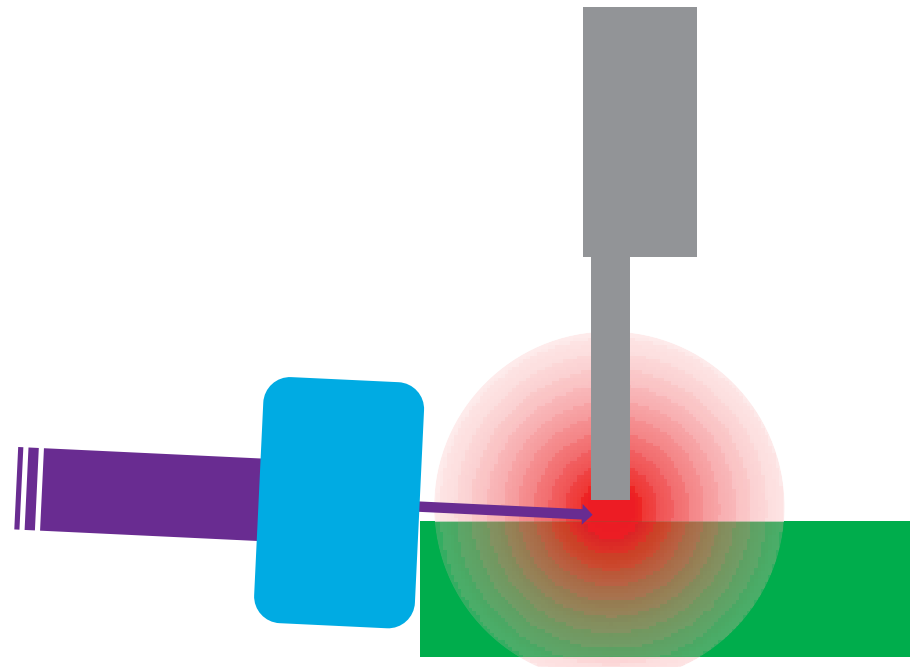
$$\phi_{critical} \approx \sqrt{2\delta}$$

$\phi_{critical}$

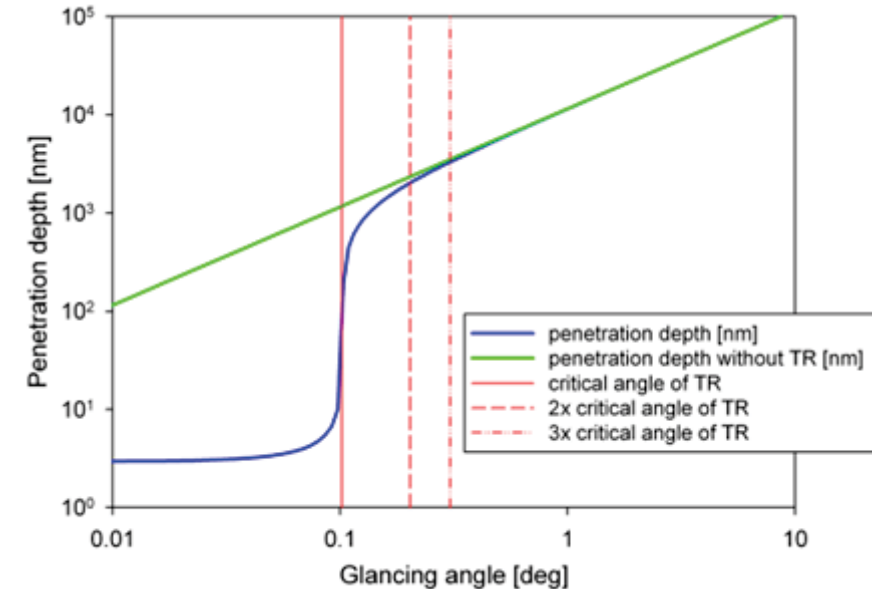
$$(Si, 17.5 \text{ keV}) \approx 0.1^\circ \approx 1.75 \text{ mrad}$$

$$(Si, 500 \text{ eV}) \approx 3.7^\circ \approx 64.6 \text{ mrad}$$



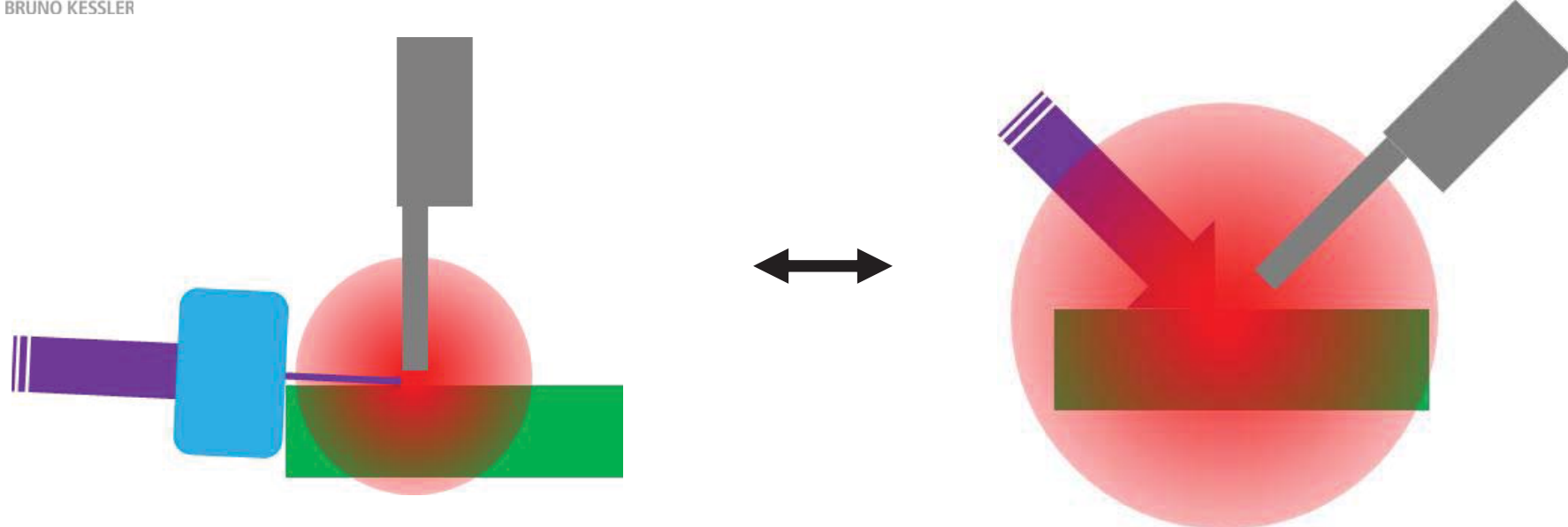


flat smooth surface (reflector)



Idea: - analyse impurities-contamination of polished surfaces

- deposit sample on a reflector and carry out analysis of the sample



- background reduction
- double excitation of sample by both the primary and the reflected beam
- small distance sample - detector ($\sim 1\text{mm}$) : large solid angle
- small sample amounts required
- detection limits in the pg range with X-ray tube excitation
- detection limits in the fg range with Synchrotron radiation excitation
- “no” matrix effects ?

e-PS, 2004, 1, 23-34

ISSN: 1581-9280

www.e-PreservationScience.org

www.Morana-rtd.com

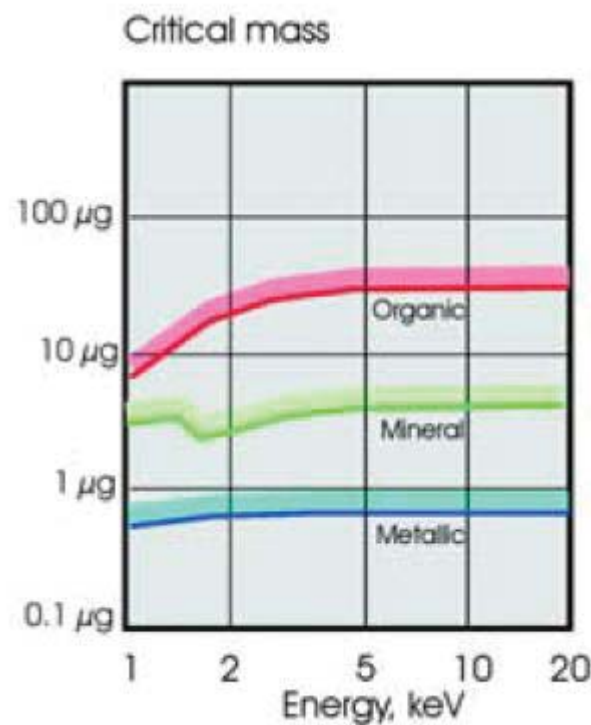
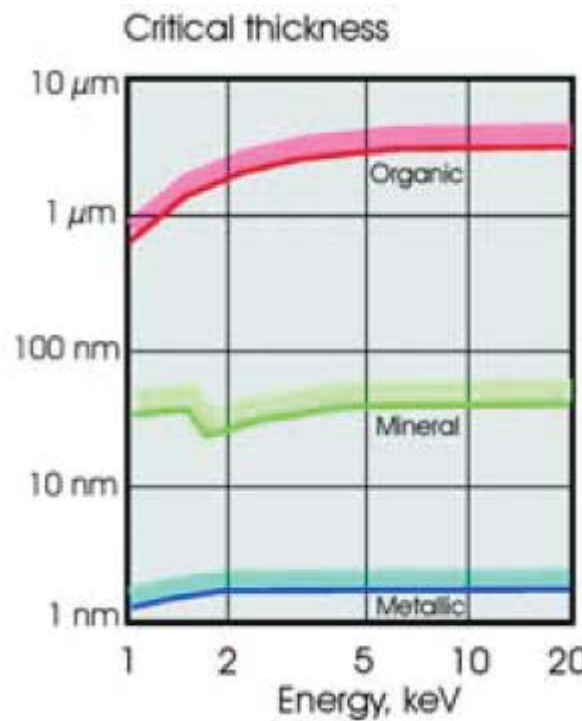
© by M O R A N A RTD d.o.o.

TOTAL REFLECTION X-RAY FLUORESCENCE SPECTROMETRY - A VERSATILE TOOL FOR ULTRA - MICRO ANALYSIS OF OBJECTS OF CULTURAL HERITAGE

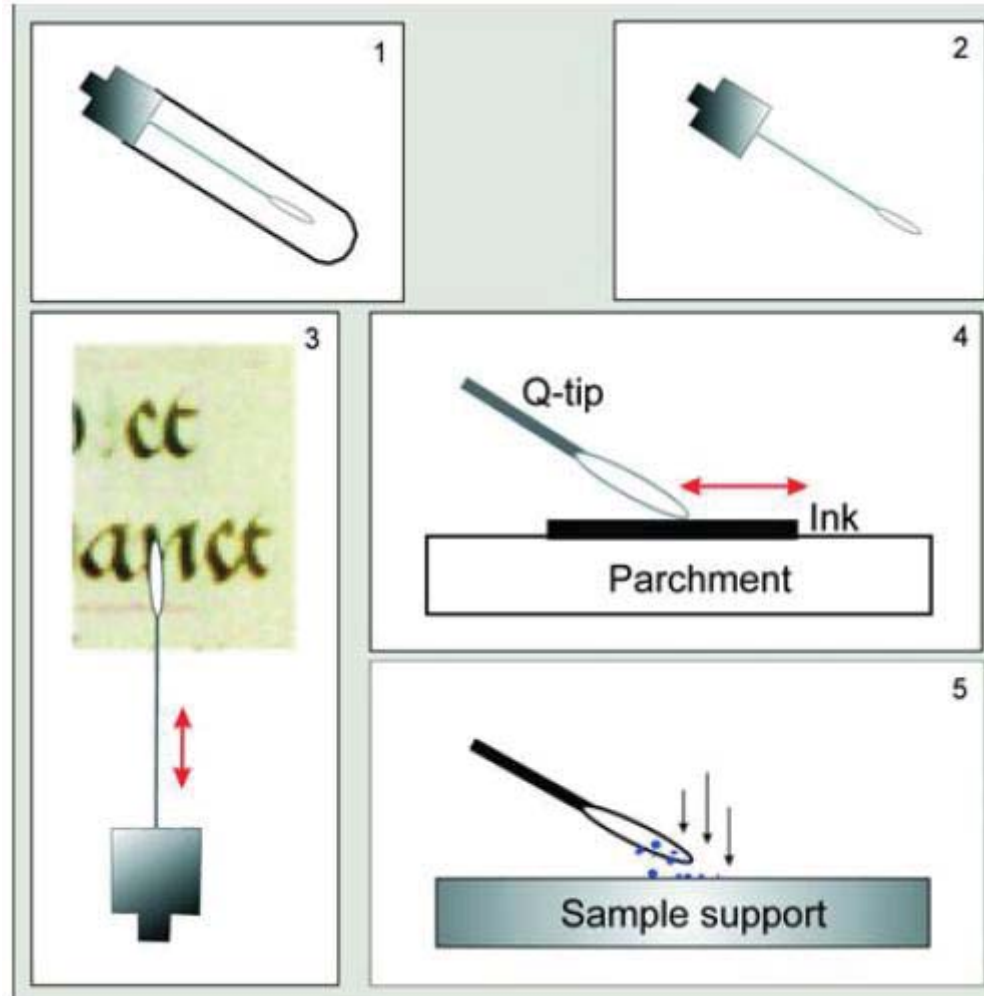
A. VON BOHLEN¹

Institute of Spectrochemistry
and Applied Spectroscopy
ISAS, Bunsen-Kirchhoff-Str. 11,
D – 44139 Dortmund, Germany

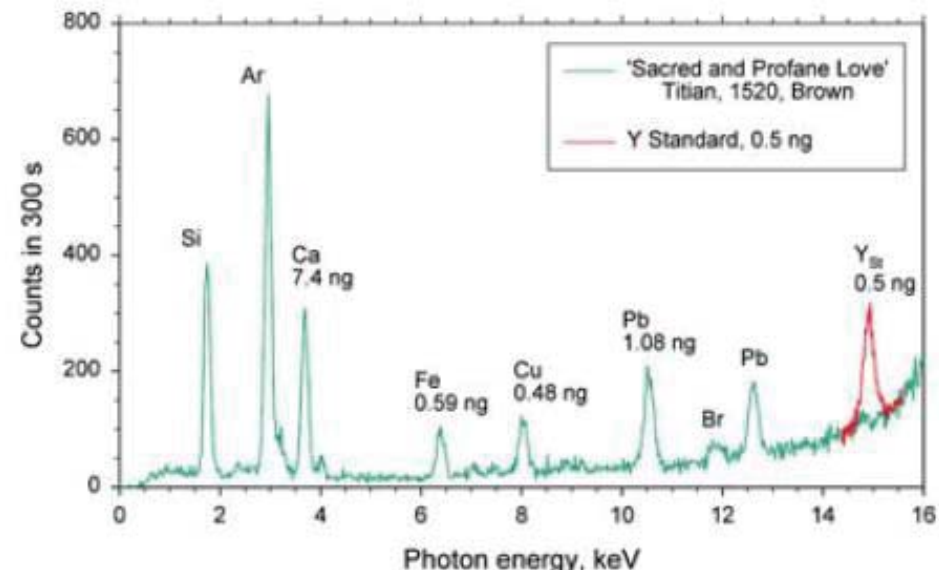
TXRF – critical thickness/mass



TXRF – cultural heritage studies - sampling



TXRF – cultural heritage studies



White Pigments

Antimony white	Sb_2O_3
Lithopone	$ZnO + BaSO_4$
Permanent white	$BaSO_4$
Titanium white	TiO_2
White lead	$2PbCO_3 \times Pb(OH)_2$
Zinc white	ZnO
Zirconium oxide	ZrO_2
Chalk	$CaCO_3$
Gypsum	$CaSO_4 \times 2H_2O$

Yellow Pigments

Auripigmentum	As_2S_3
Cadmium yellow	CdS
Chrome yellow	$2PbSO_4 \times PbCrO_4$
Cobalt yellow	$K_3[Co(NO_2)_6] \times 1.5H_2O$
Lead-tin yellow	$Pb_2SnO_4 / PbSn_2SiO_7$
Massicot	PbO
Naples yellow	$Pb(SbO_3)_2 / Pb_3(SbO_4)_2$
Strontium yellow	$SrCrO_4$
Titanium yellow	$NiO \times Sb_2O_3 \times 20TiO_2$
Yellow ochre	$Fe_2O_3 \times nH_2O$ (20% - 70%)
Zinc yellow	$K_2O \times 4ZnO \times 4CrO_3 \times 3H_2O$

Red Pigments

Cadmium red	Cadmium red
Cadmium vermillion	Cadmium vermillion
Chrome red	Chrome red
Molybdate red	Molybdate red
Realgar	Realgar
Red lead	Red lead
Red ochre	Red ochre
Vermilion	Vermilion

Green Pigments

Basic copper sulfate	$Cu_x(SO_4)_y(OH)_z$
Chromium oxide	Cr_2O_3
Chrysocolla	$CuSiO_3 \times nH_2O$
Cobalt green	Cobalt green
Emerald green	Emerald green
Guignet green	Guignet green
Malachite	Malachite
Verdigris	Verdigris

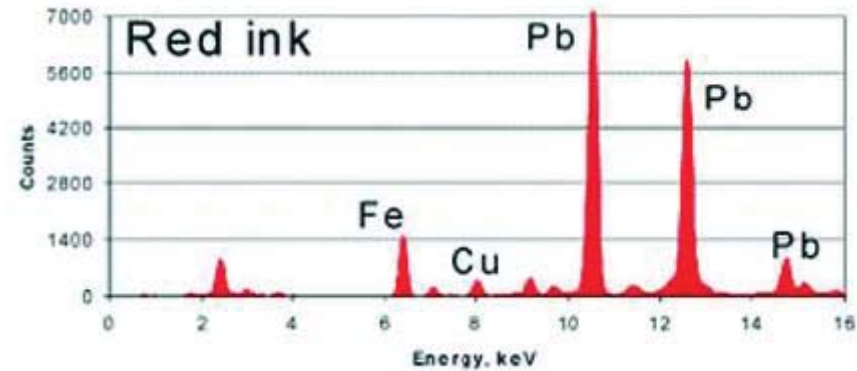
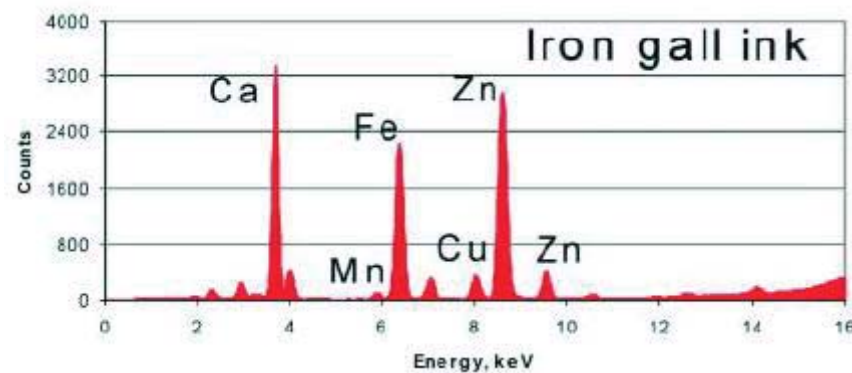
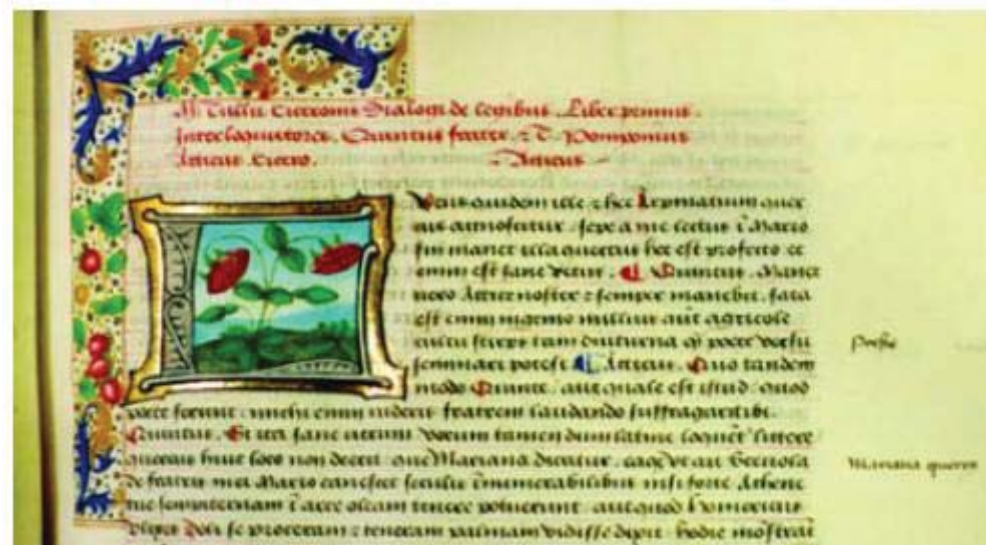
Blue Pigments

Azurite	$2CuCO_3 \times Cu(OH)_2$
Cerulean blue	$CoO \times nSnO_2$
Cobalt blue	$CoO \times Al_2O_3$
Cobalt violet	$Co_3(PO_4)_2$
Egyptian blue	$CaO \times CuO \times 4SiO_2$
Manganese blue	$BaSO_4 \times Ba_3(MnO_4)_2$
Prussian blue	$Fe_4[Fe(CN)_6]_3$
Smalt	Co-glass ($K_2O + SiO_2 + CoO$)
Ultramarine	$Na_{8..10}Al_6Si_6O_{24}S_{2..4}$

Black Pigments

Antimony black	Sb_2O_3
Black iron oxide	$FeO \times Fe_2O_3$
Carbon black	C (95%)
Cobalt black	CoO
Ivory black	$C + Ca_3(PO_4)_2$
Manganese oxide	$MnO + Mn_2O_3$

TXRF – cultural heritage studies



TXRF – cultural heritage studies

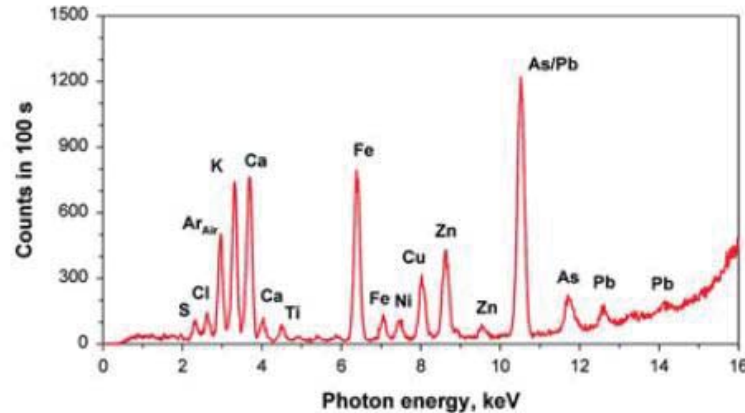


Figure 11. Scroll of a Cello made by L. Maugin, 19th century and TXRF spectrum of the original varnish.

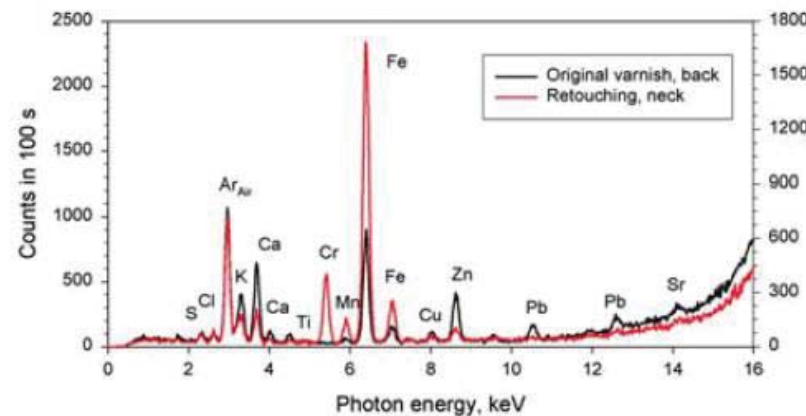
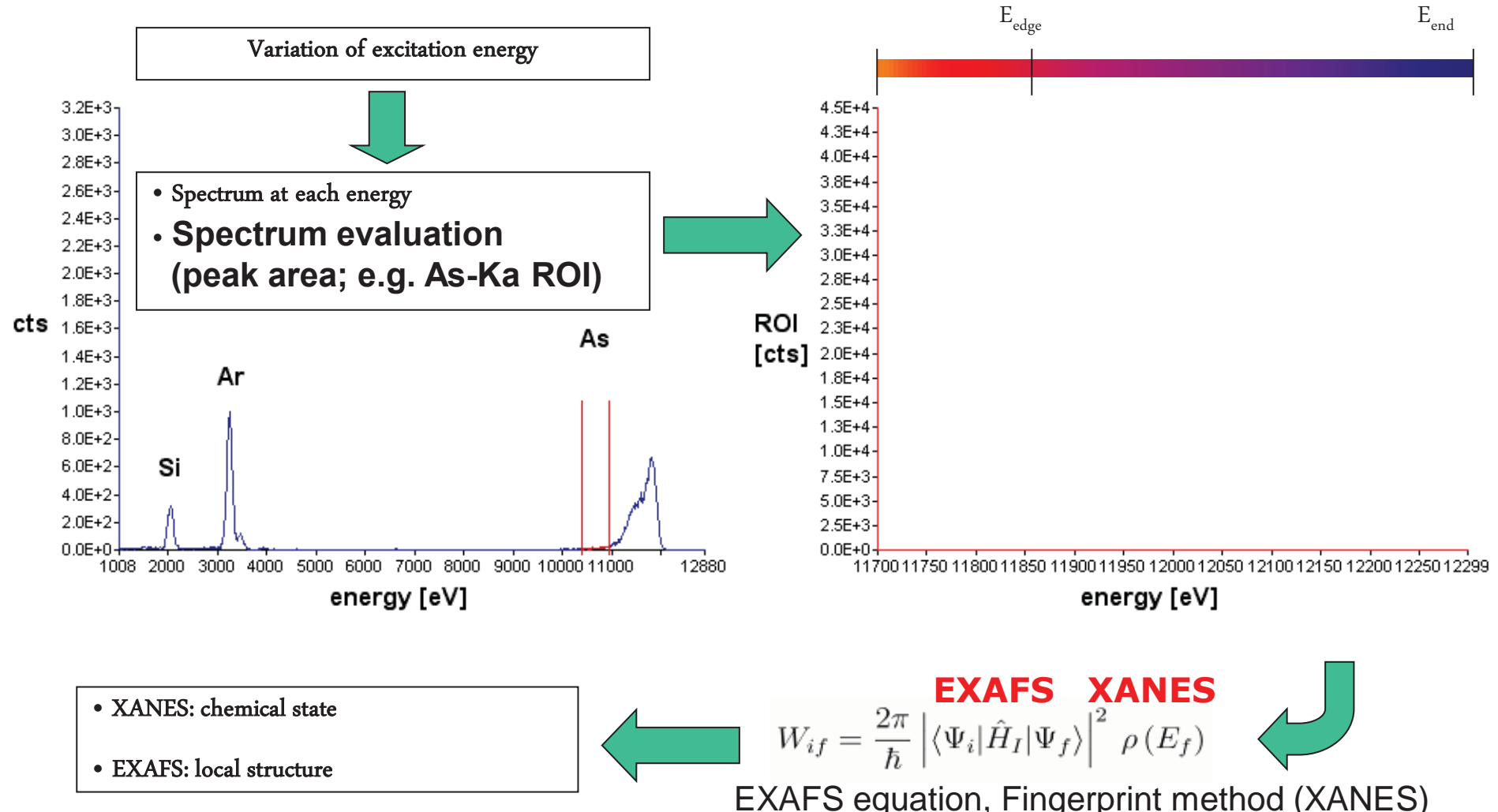


Figure 12. TXRF spectra of an original and retouched violin varnish from a violin made by Th. & S. Thompson, London, about 1780.

The measurement: Example – TXRF-XANES of As droplet sample on Si reflector



Arsenic speciation in cucumber (*Cucumis sativus* L.) xylem sap by K-edge TXRF-XANES

Giancarlo Pepponi

**C. Streli, P. Wobrauschek, F. Meirer,
V.G. Mihucz, G. Zaray, V. Czech,
J. Broekaert, U. Fittschen
and G. Falkenberg**

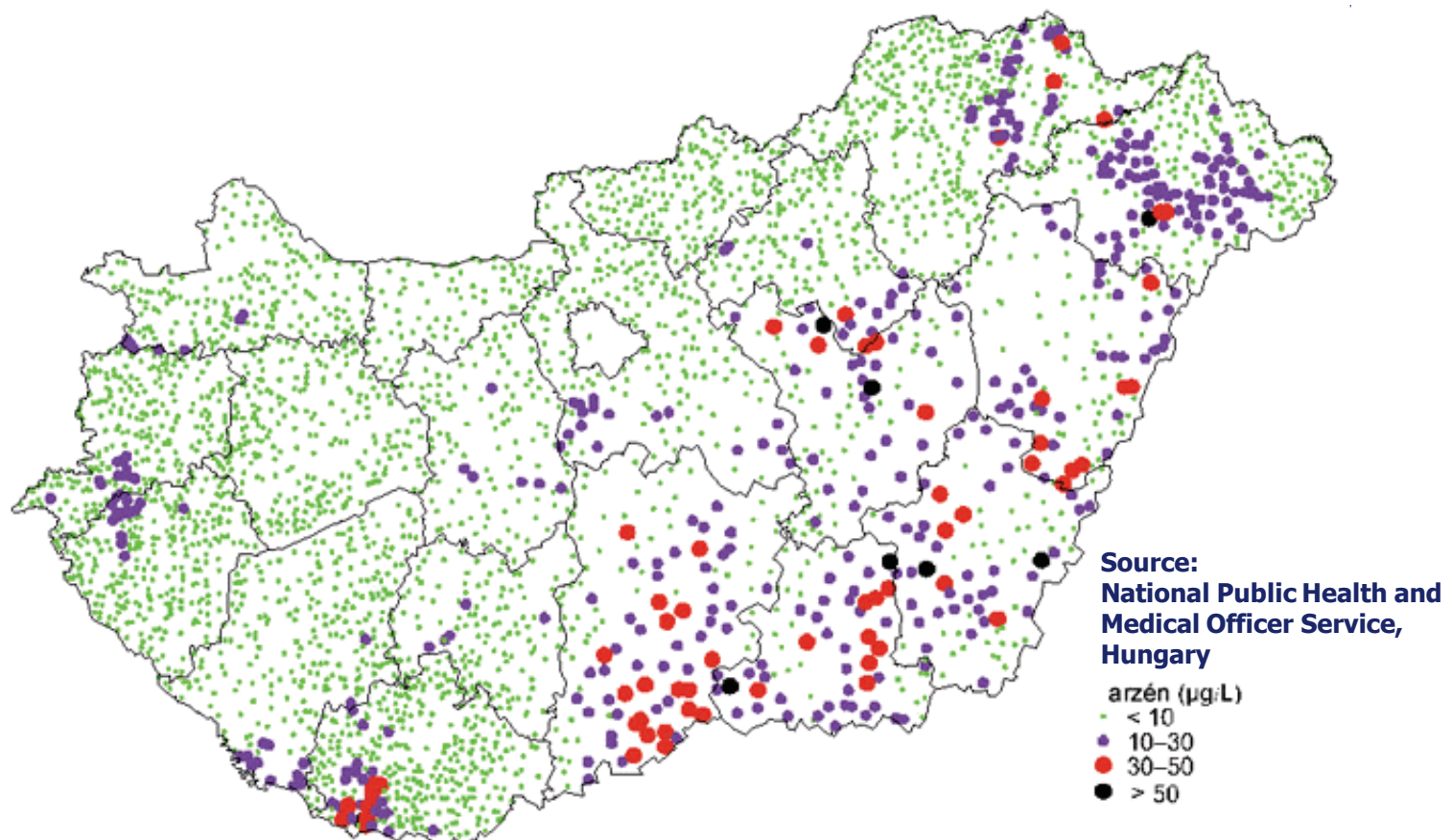
Application of synchrotron-radiation-induced TXRF-XANES for arsenic speciation in cucumber (*Cucumis sativus* L.) xylem sap

F. Meirer, G. Pepponi, C. Streli, P. Wobrauschek, V. G. Mihucz, G. Záray, V. Czech, J. A. C. Broekaert, U. E. A. Fittschen, G. Falkenberg

X-Ray Spectrometry, Volume 36, Issue 6, pages 408–412, 2007

Cucumber xylem sap - motivation

- Arsenic is contained in groundwater in Eastern Hungary in concentrations that can exceed 50 µg/L



Cucumber xylem sap - motivation

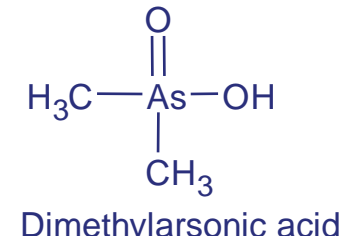
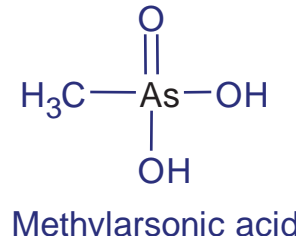
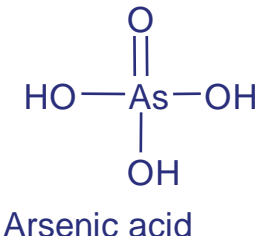
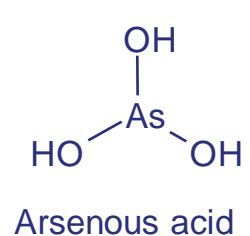
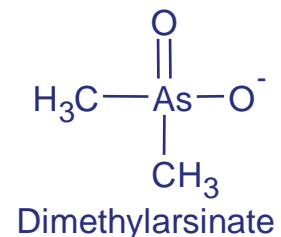
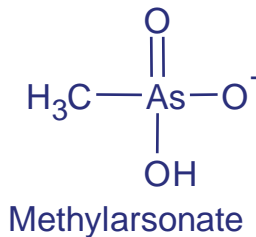
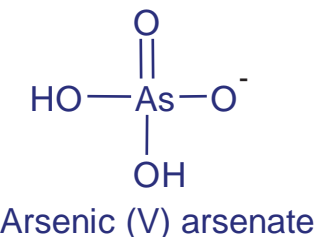
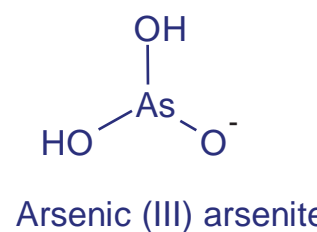
- different species of As have different toxicity

Compound	LD ₅₀ mg/kg
As ₂ O ₃	20
Na ₃ AsO ₃	60
Na ₃ AsO ₄	120
CH ₃ AsO(OH) ₂ (MMA)	700
CH ₃ AsO(ONa) ₂	1800
(CH ₃) ₂ AsO(OH) (DMA)	1600
(CH ₃) ₂ AsO(ONa)	2600
(CH ₃) ₃ As ⁺ CH ₂ COO ⁻ (As-betaine; AsB)	4500

Cucumber xylem sap - motivation

Occurrence of As species in plants, lichens, fungi, algal species and microorganisms

Source: V.M. Dembitsky, T. Rezanka, Plant Science 165, 2003, 1177-1192



Speciation of the As is important to . . .

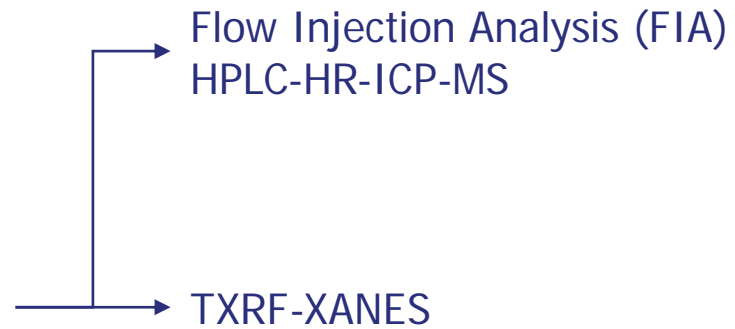
- understand how plants metabolise and transform As
- assess the health risk caused by As entering the food chain

In aerobic soils arsenate [As(V)] is the most stable form

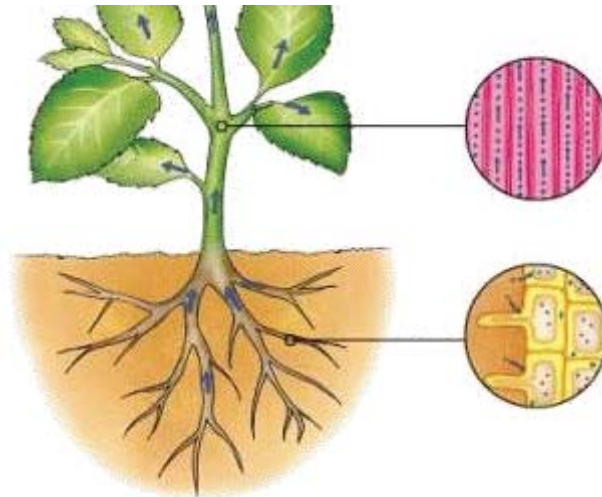
Cucumber xylem sap - experimental



- At two leaf stage:
transferred in solution with arsenic compounds
and diminished phosphate concentration
- After 30 days from germination (17 d arsenic):
 - stem cut 2 mm above root neck
 - sap collected with micropipettes for 1 hour
into PE vials immersed in ice salt bath



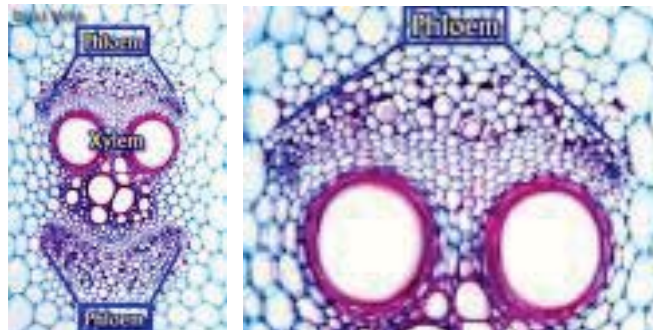
Cucumber xylem sap - experimental



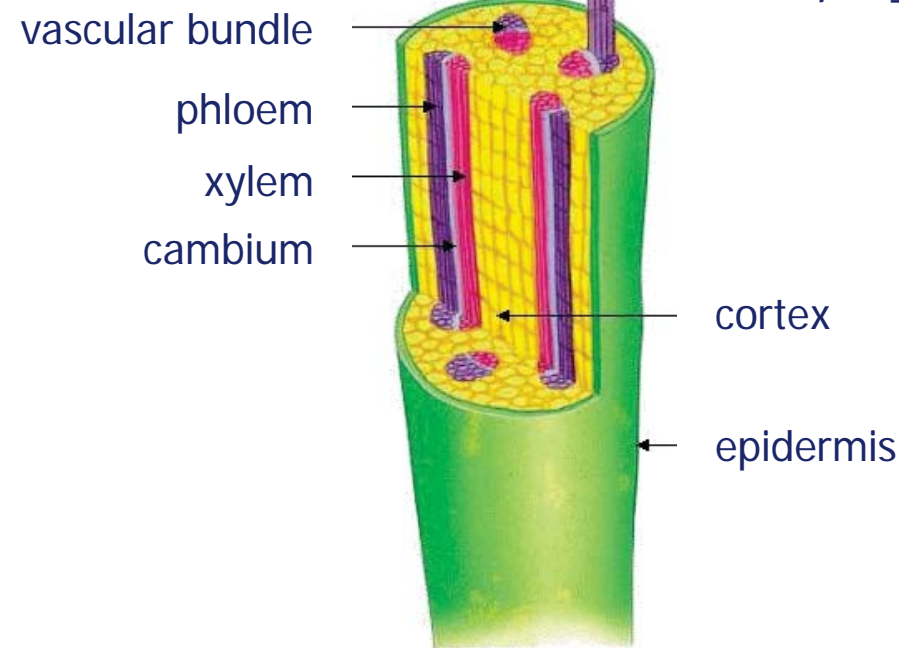
water is “pulled up” through the xylem

water is taken in through the roots

cucumber vascular bundle



Source:
[http://www.botany.hawaii.edu/faculty/webb/
BOT410/410Labs/LabsHTML-
99/Xylem/Labxyphlo99.html](http://www.botany.hawaii.edu/faculty/webb/BOT410/410Labs/LabsHTML-99/Xylem/Labxyphlo99.html)



Source:
[http://www.fairchildgarden.org/
EduProfDev/Leaf_anatomy.html](http://www.fairchildgarden.org/EduProfDev/Leaf_anatomy.html)

Cucumber xylem sap - experimental

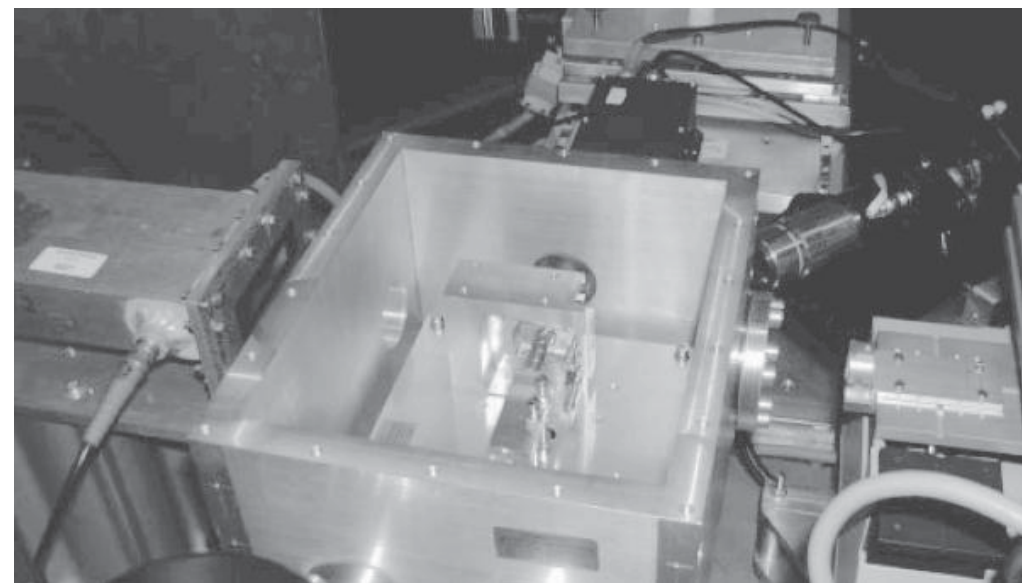
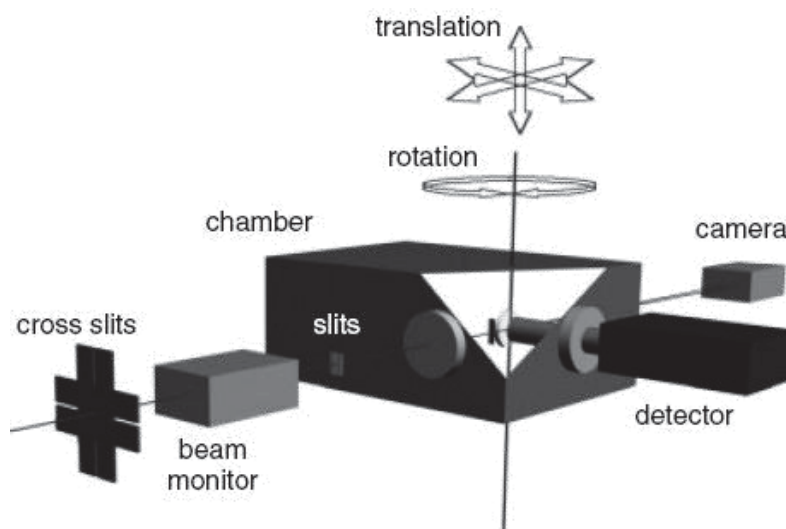
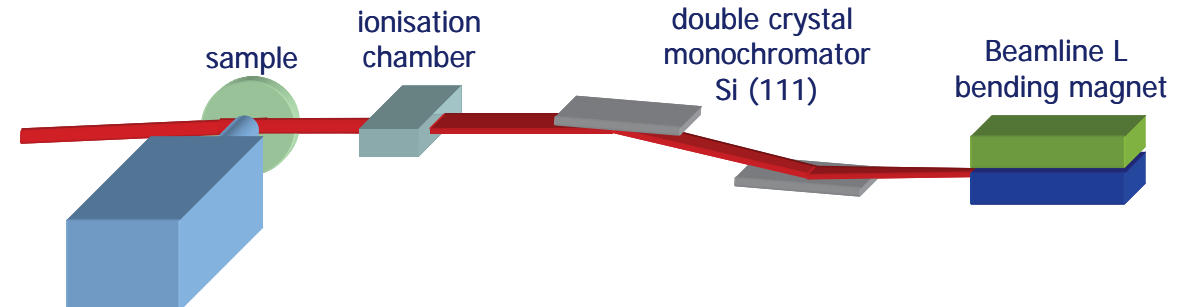
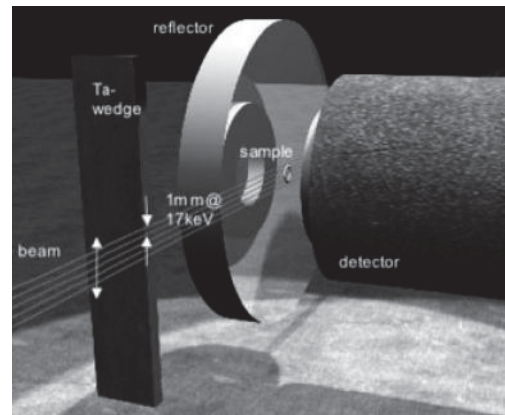
Solutions were

pipetted onto quartz reflectors
 vacuum dried
 sent in inert atmosphere (Ar)

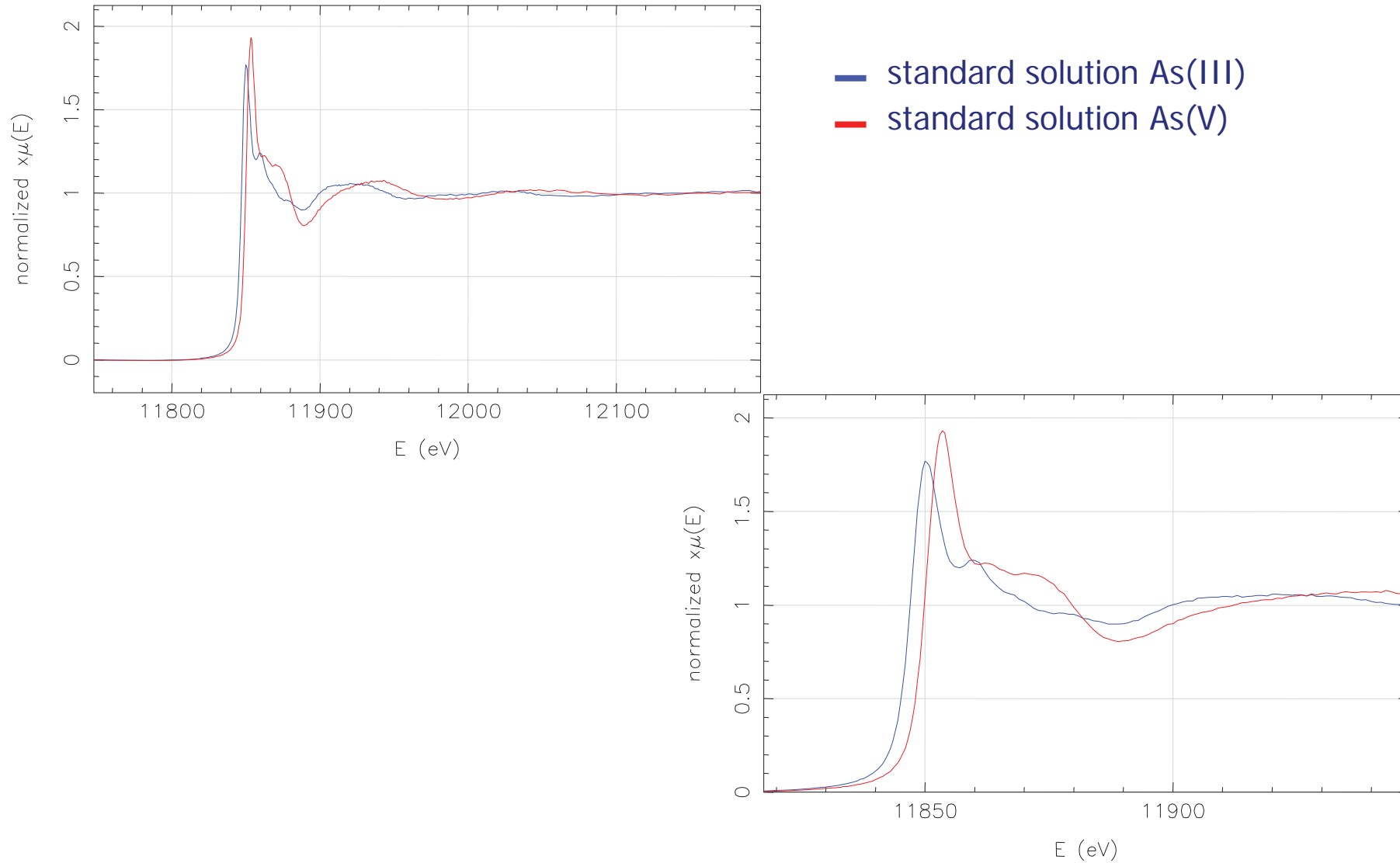


reflector	sample	oxidation number	concentration [ppb]	volume [μl]	mass As [ng]
117	standard solution	3	10000	20	200
122	nutrient solution	3	150	20	3
101	nutrient solution	3	150	10	1.5
124	xylem sap	3	50	20	1
121	standard solution	5	10000	20	200
123	nutrient solution	3	150	20	3
115	xylem sap	5	30	10	0.3

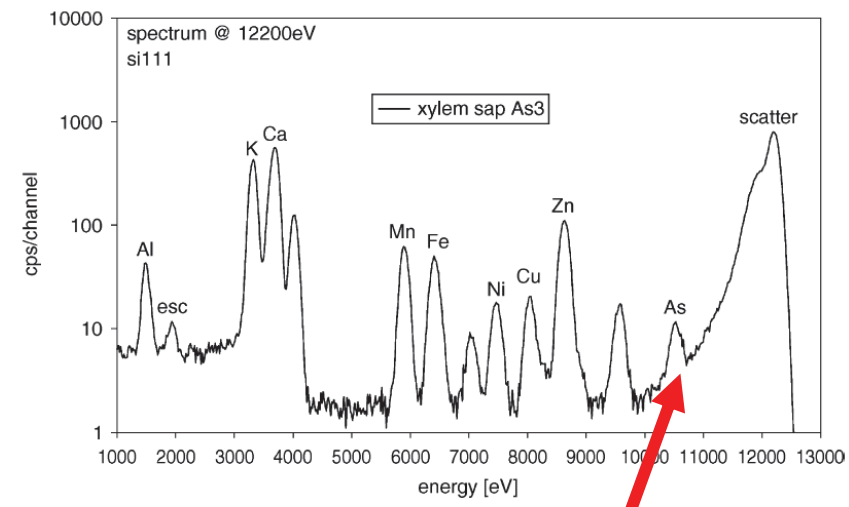
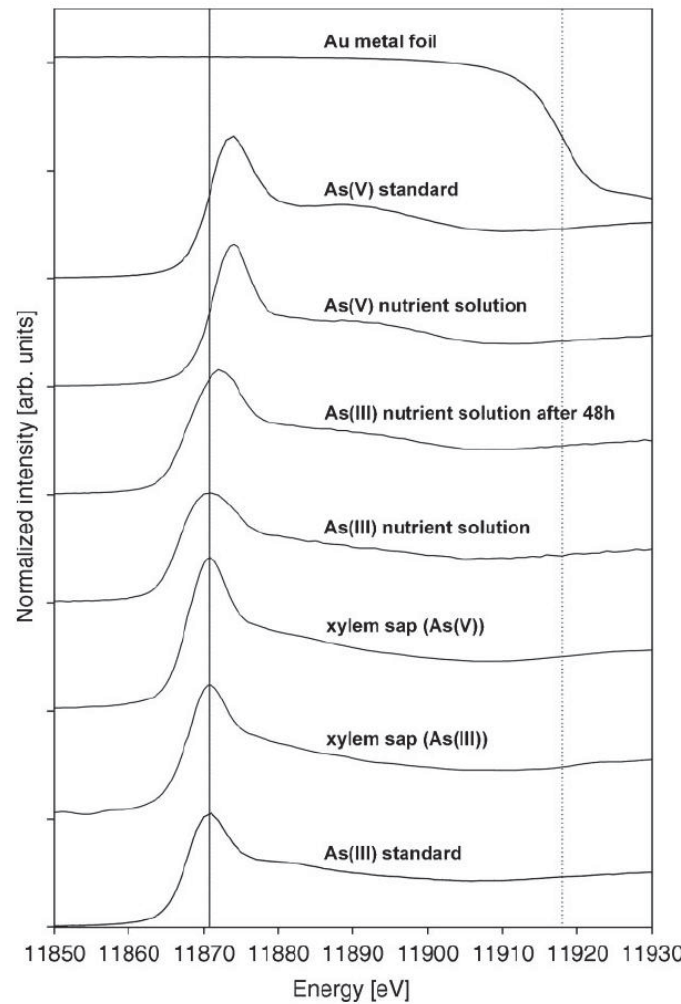
HASYLAB L - setup



As standard solutions - XANES



Fluorescence signal extraction



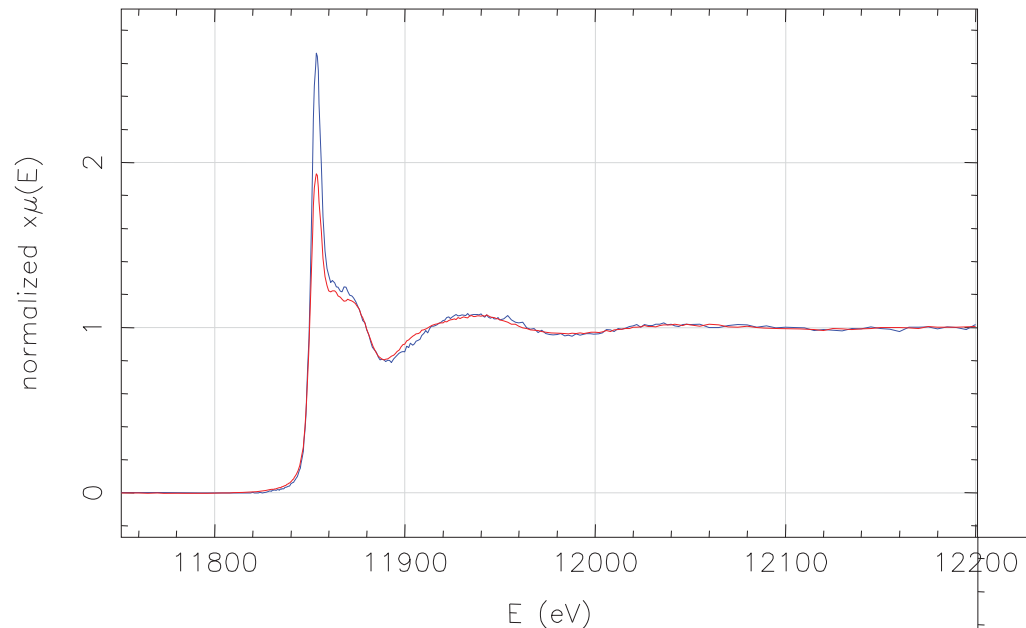
Results:

- Speciation of As was possible down to the 30ppb level
- As(III) in nutrient solutions oxidises easily to As(V)
- Cucumber roots convert As(V) to As(III)

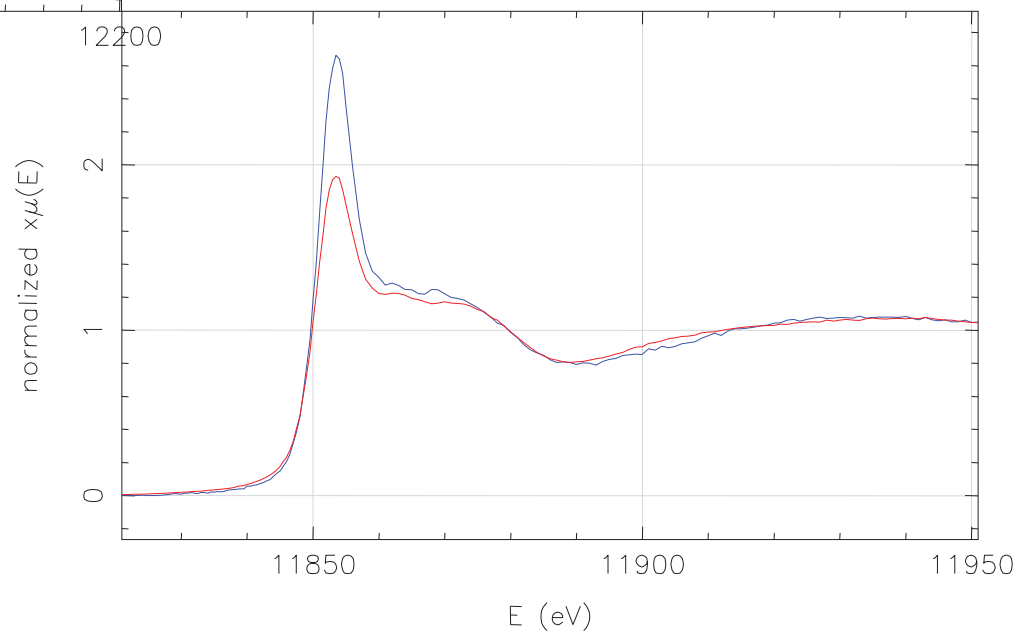
Sample	As(III) [%]	As(V) [%]	R-factor	χ^2	reduced χ^2
xylem sap (As(III))	88 ± 3	12 ± 3	0.0155	1.09	0.0115
xylem sap (As(V))	83 ± 3	17 ± 3	0.0143	1.06	0.0112
As(III) nutrient solution	100 ± 3	0 ± 3	0.0103	0.68	0.0072
As(III) nutrient solution after 48h	71 ± 3	29 ± 3	0.0080	0.60	0.0063
As(V) nutrient solution	2 ± 2	98 ± 2	0.0065	0.63	0.0066

F. Meirer et al., X-Ray Spectrometry 36 (2007) 408-412.

A strange? result

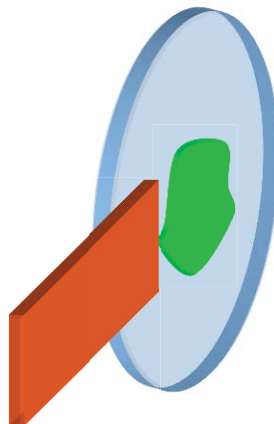


- nutrient solution As(V)
- standard solution As(V)



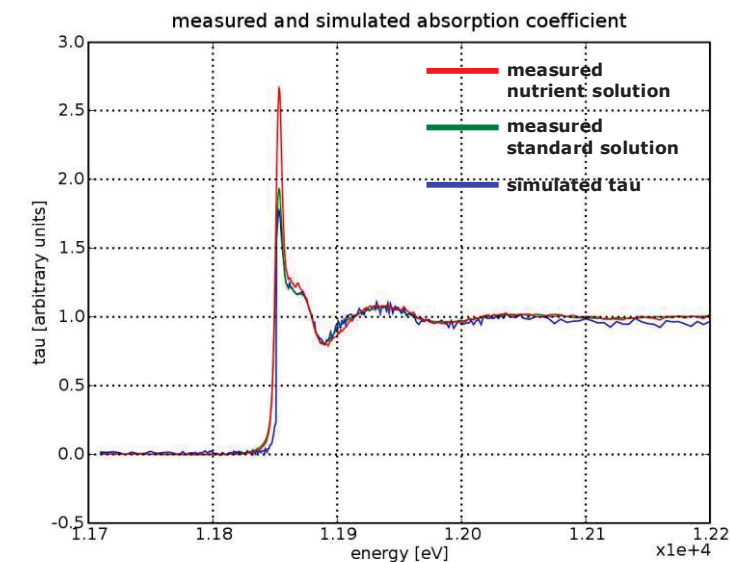
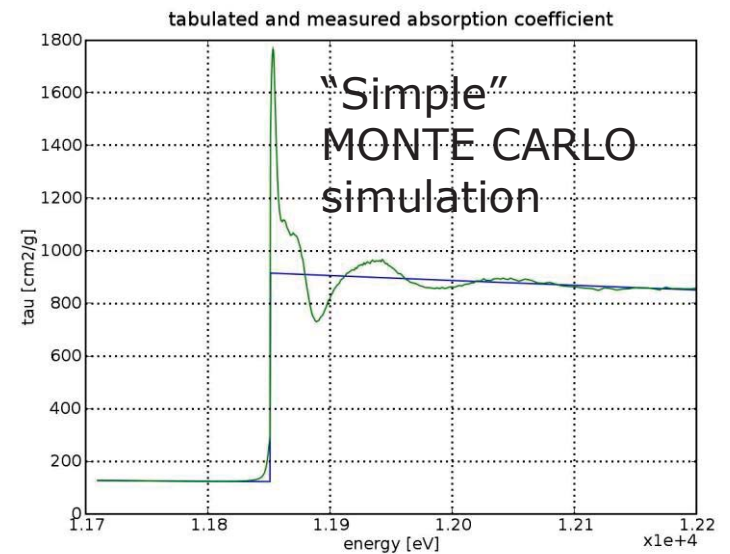
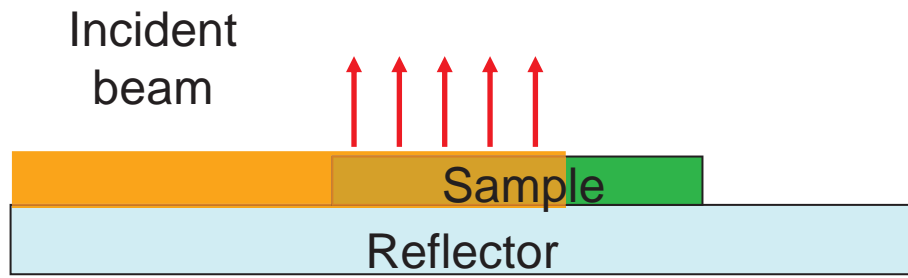
Self Absorption

$$I(x) = I_0 \exp(-\mu x)$$

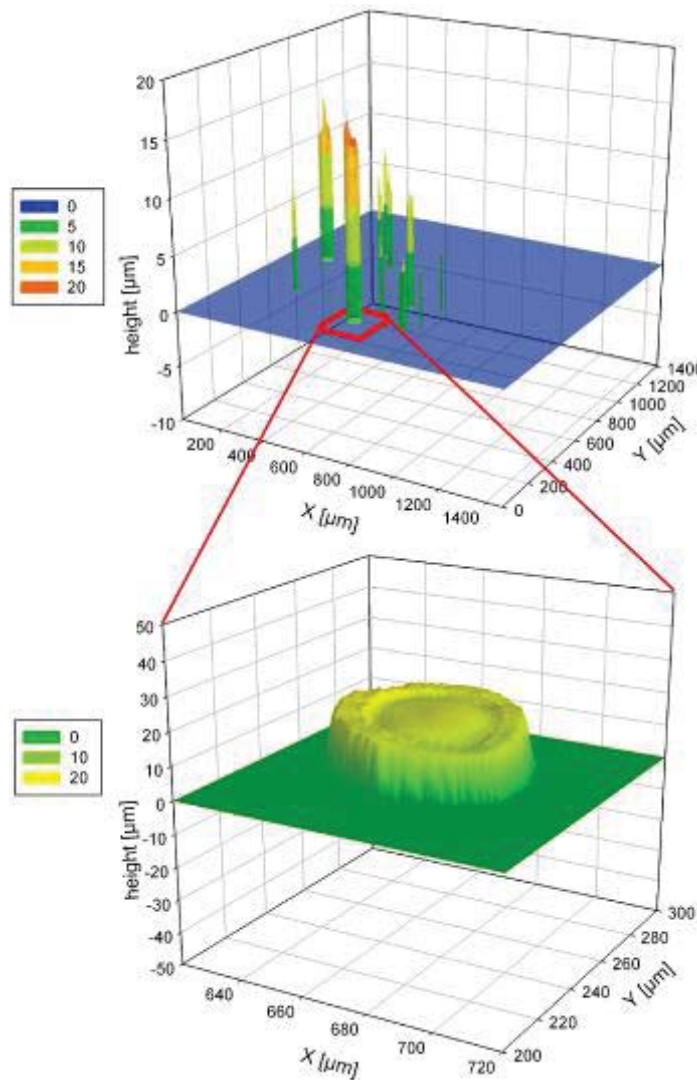


Sample (droplet) size becomes thickness, i.e. path that the primary beam crosses

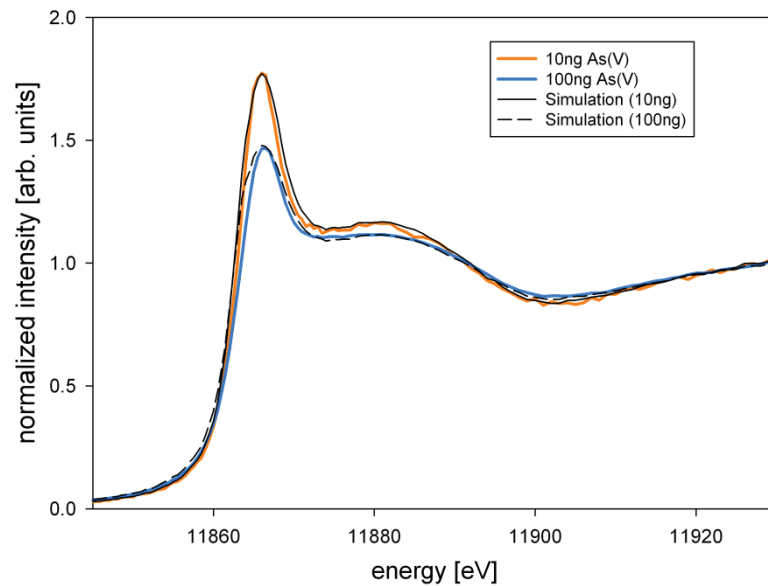
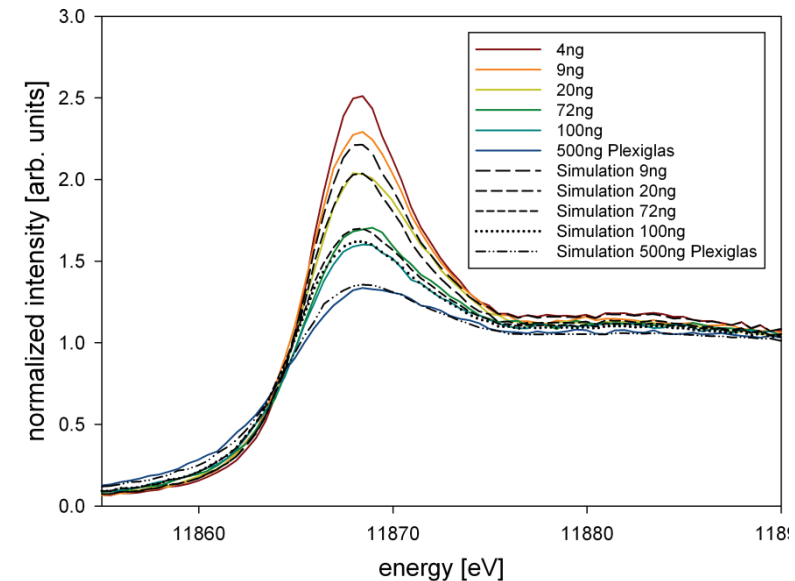
⇒ Large or highly concentrated samples: penetration depth of incident beam < sample size



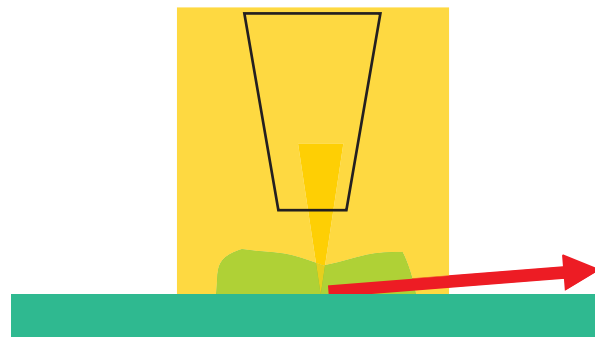
Self Absorption



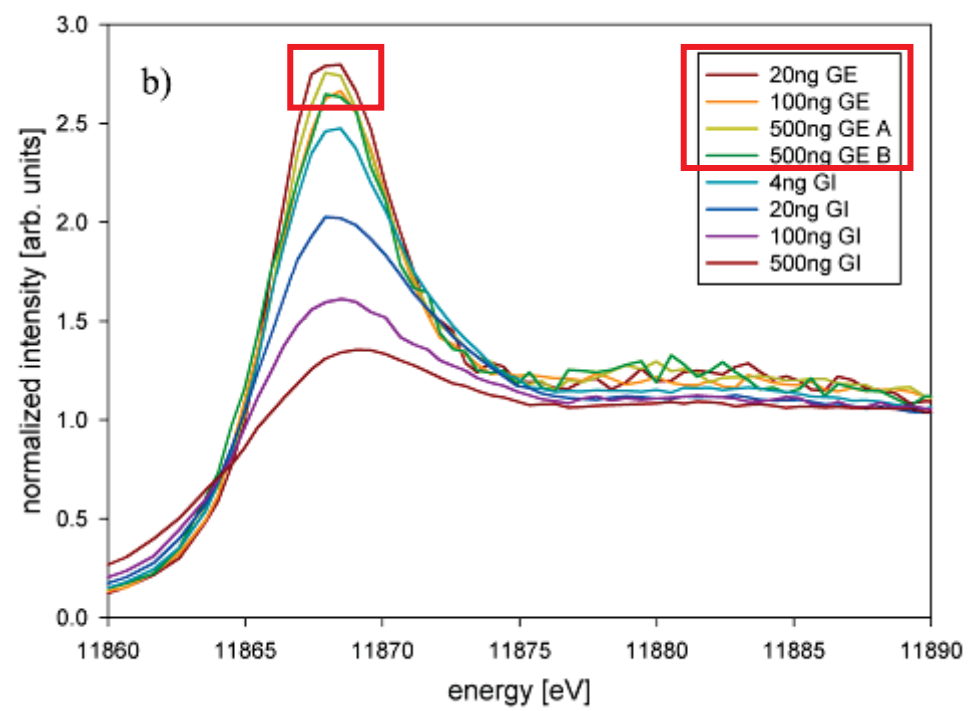
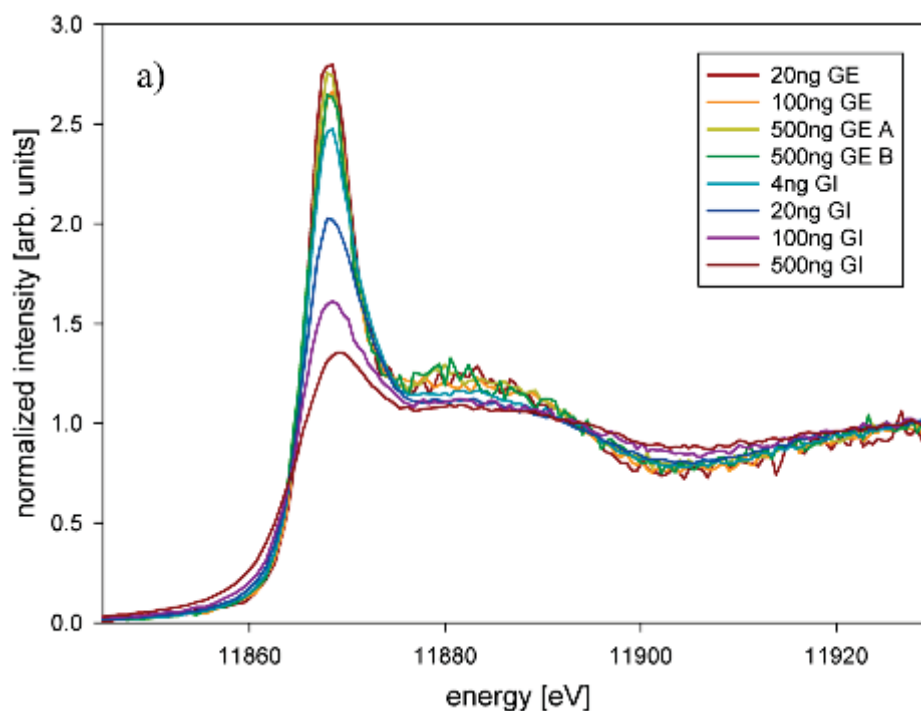
F. Meirer et al., Spectrochimica Acta Part B
63 (2008) 1496–1502



Self Absorption – grazing exit



- GE setup suffers minimally from self-absorption effects
- Shows lower sensitivity than GI-setup
 ⇒ difficult to apply to XAFS analysis of trace amounts (few nanograms) of samples



F. Meirer et al., J. Appl. Phys. 105, 074906 (2009)

Speciation of copper and zinc in size-fractionated aerosol samples using TXRF-XANES

**J. Osán¹, F. Meirer^{2,3}, S. Török¹, D. Ingerle²,
C. Streli² and G. Pepponi⁴**

¹KFKI Atomic Energy Research Institute, P.O. Box 49, H-1525 Budapest, Hungary; osan@aeki.kfki.hu,

²Atominstitut, Vienna Univ. of Technology, Stadionallee 2, A-1020 Vienna, Austria

³Stanford Synchrotron Radiation Lightsource, SLAC National Accelerator laboratory, 2575 Sand Hill Road, Menlo Park CA 94025, USA

⁴Fondazione Bruno Kessler, Via Sommarive 18, I-38123 Povo, Italy

**János Osán, Florian Meirer, Veronika Groma, Szabina Török, Dieter Ingerle,
Christina Streli, Giancarlo Pepponi**

Speciation of copper and zinc in size-fractionated atmospheric particulate matter using total reflection mode X-ray absorption near-edge structure spectrometry

Spectrochimica Acta Part B 65 (2010) 1008–1013

ICTP-IAEA -2011 - Trieste – SR -(micro)XRF – Giancarlo Pepponi

Particulate matter - motivation

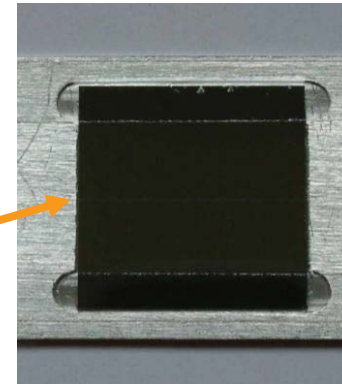
- Health effects of aerosol depend on the size distribution and the chemical composition of the particles
- Heavy metals of anthropogenic origin are connected to the fine ($PM_{2.5}$) aerosol fraction
- Determination of copper and zinc speciation in size-fractionated aerosols from a short sampling period
- Relation of the size distribution of Cu and Zn speciation to the aerosol sources

Size fractioned aerosol sampling

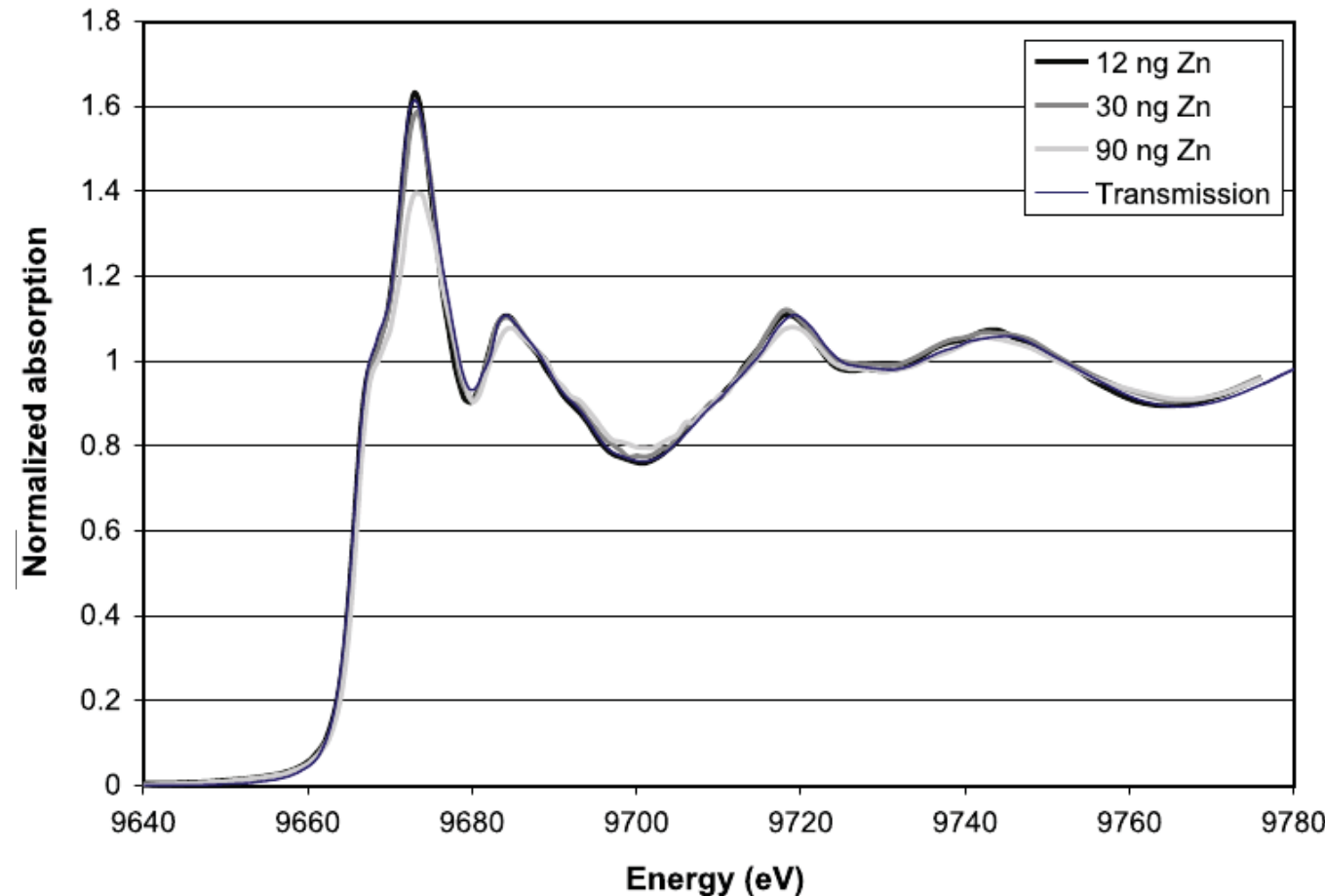
- 7-stage May-type cascade impactor
- cut-off diameters: 16, 8, 4, 2, 1, 0.5, 0.25 μm for stages 1–7 at 20 lpm flow rate
- sampling 20–3200 l air depending on stages and aerosol concentration



The deposited aerosol particles form a 200–500 μm wide strip in the middle of the Si wafer of 20x20 mm²



Particulate matter – self absorption



Particulate matter – Zn XANES

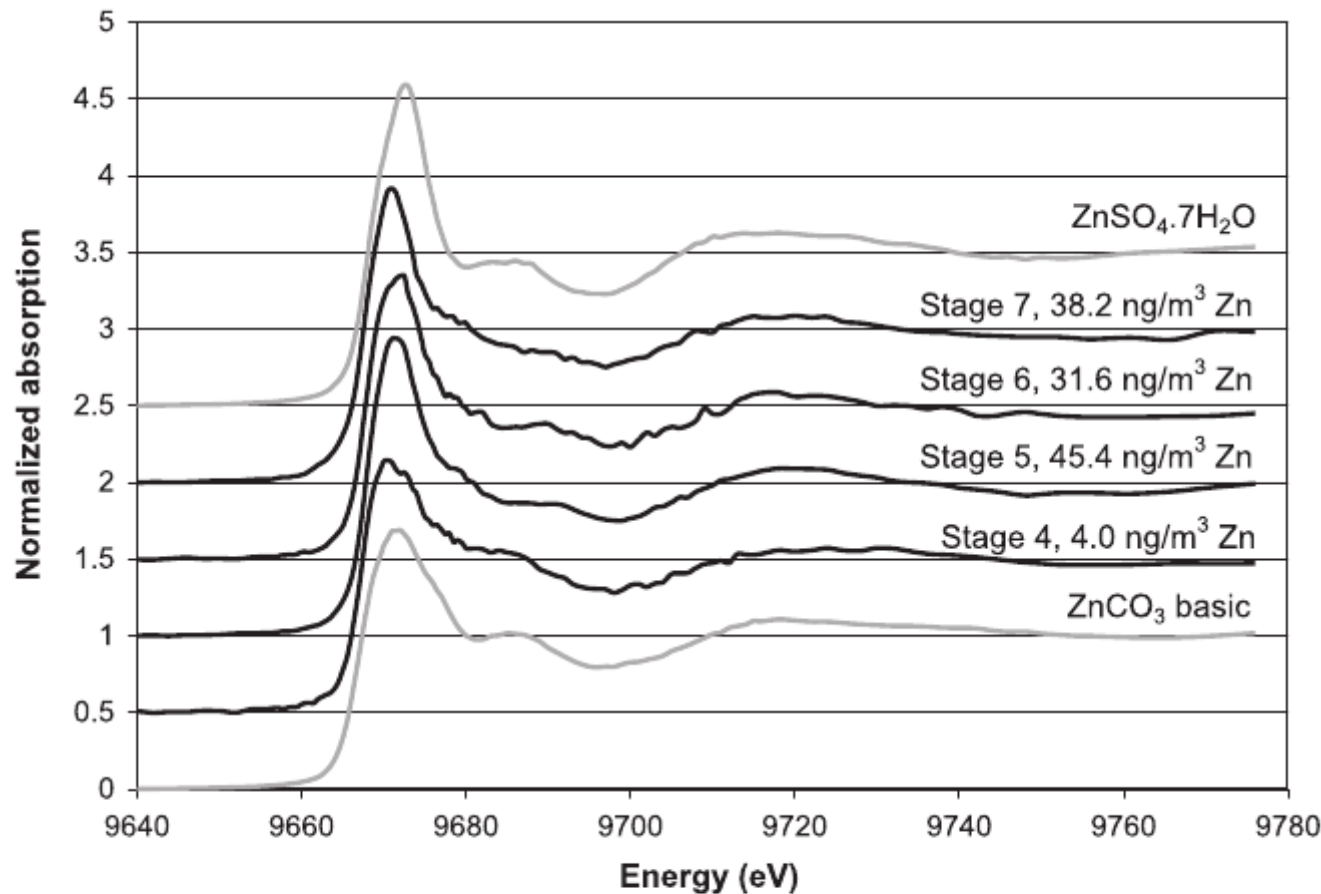


Fig. 5. Zn–K edge TXRF-XANES spectra of the aerosol sample set collected at the airport of Budapest on 12 01 2006; zinc sulfate and carbonate standard spectra are plotted for comparison.

Particulate matter – Cu XANES

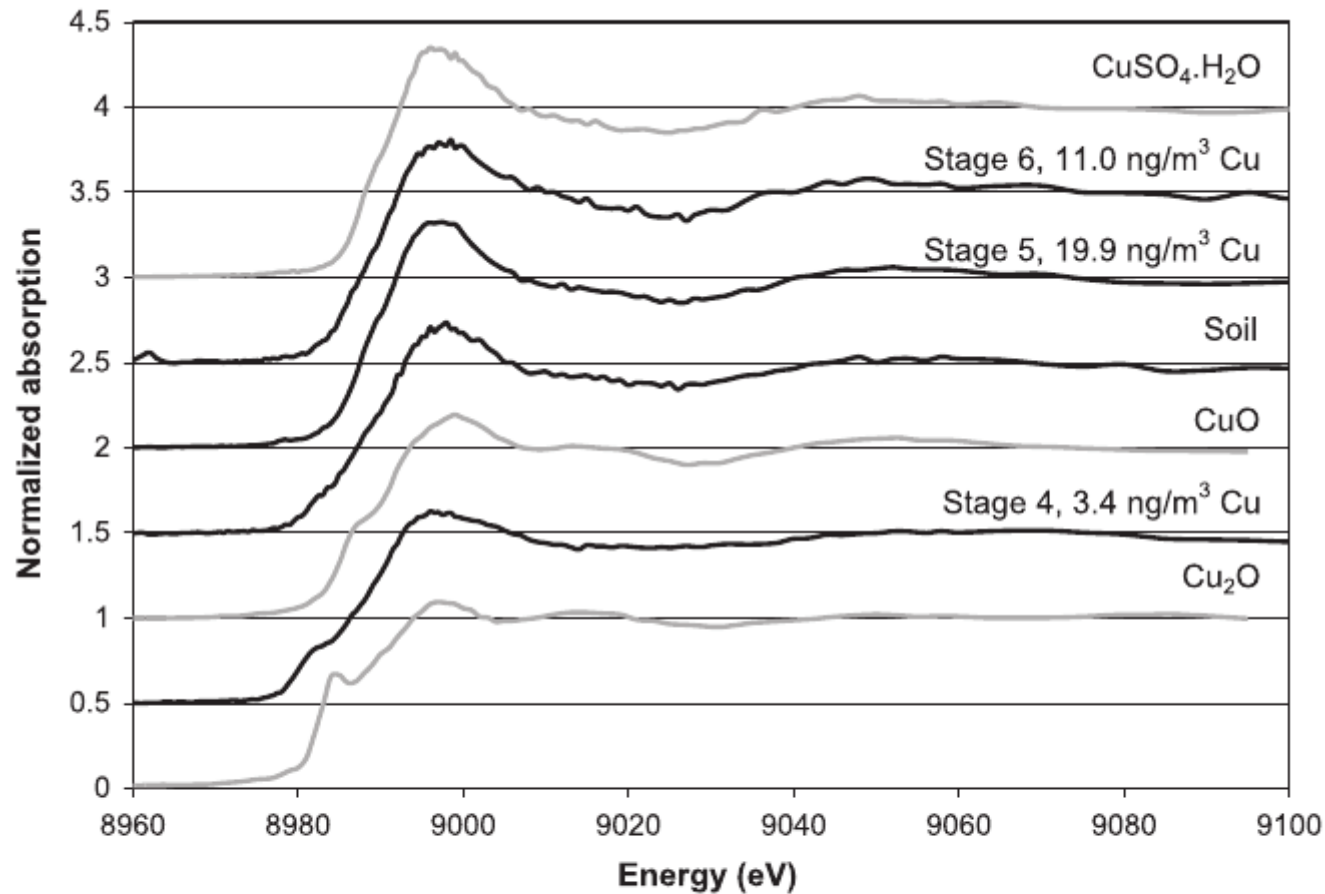


Fig. 6. Cu–K edge TXRF-XANES spectra of the aerosol sample set collected at the airport of Budapest on 12 01 2006; standard spectra of Cu(II) sulfate, Cu(II) oxide and Cu(I) oxide are plotted for comparison.

Particulate matter – conclusions

The combination of TXRF-XANES and direct sampling of aerosol particles onto Si wafers using a May-type cascade impactor was found to be well applicable for non-destructive speciation of transition metals in atmospheric particulate matter.

Cu and Zn chemical forms could be identified from air concentrations as low as 140 pg/m³ for a collected air volume of 1 m³ (50 min sampling time).

Speciation of metals with air concentrations in the ng/m³ range is possible in the time scale of a few minutes, allowing the tracing of mobile sources variable in time.

Cu and Zn were found to be bound to secondary aerosol particles in the form of sulfates and nitrates in the fine fraction.

Sources of soil resuspension and brake pad wear erosion could be distinguished based on the chemical form of copper in the coarse fraction (2µm).

TXRF XANES conclusions

TXRF XANES good for:

- small sample amount (mass)
- diluted samples
- solutions/suspensions
- particulate matter

Speciation performed down to:

- 30 ng/ml (xylem sap)
- 140 pg/m³ (fine particulate matter)

Weaknesses:

- self absorption in “highly” concentrated samples (standards)
- alignment can be time consuming